Table 1
Number of the reported cases of bacterial meningitis, which occurred in children less than 16 years old in Hokkaido prefecture during recent four years of period.

Year	Hib	S. pn	GBS	E. coli	Others	Total
2007	11 (6/5)	6 (4/2)	2 (1/1)	1 (1/0)	1 (0/1)	21 (12/9)
2008	13 (7/6)	1 (1/0)	2 (1/1)	1 (1/0)	1 (1/0)	18 (11/7)
2009	12 (8/4)	4 (1/3)	1 (1/0)	2 (1/1)		19 (11/8)
2010	11 (5/6)	4 (1/3)	0	1 (0/1)		16 (6/10)
Total	47 (26/21)	15 (7/8)	5 (3/2)	5 (3/2)	2 (1/1)	74 (40/34)

Numbers in parentheses are (male/female). Hib, Haemophilus influenzae type b; S. pn, Streptococcus pneumoniae; GBS, group B Streptococcus; E. coli, Escherichia coli.

4. Introduction of the H. influenzae type b conjugate vaccine and the pediatric 7-valent pneumococcal conjugate vaccine in Japan

The H. influenzae type b conjugate vaccine and the pediatric 7-valent pneumococcal conjugate vaccine were introduced in Japan in 2008 and 2010, respectively. I worked as a member of some groups, which accumulated the basic data on the occurrence of bacterial meningitis in Japan and urged the government to introduce those vaccines. Number of cases of bacterial meningitis, which occurred in children in Hokkaido during recent four years of period, are shown in Table 1. To accumulate this kind of data is sober and important in evaluating the efficacy of the H. influenzae type b conjugate vaccine and the pediatric 7-valent pneumococcal conjugate vaccine. I honestly hope that the figures in Table 1 will be rewritten as zero in the future.

Acknowledgements

Fig. 7. Postmortem histological findings of influenza-associated encephalopathy. A; Brain (medulla) tissue showing vasogenic edema with hydropic degeneration, hyalinization of vessels, and extravasation of plasma proteins (hematoxylin–eosin staining). B; Lung tissue showing interstitial pneumonia and microvascular thrombi (hematoxylin–eosin staining).

which, initially even Japanese pediatricians outside Hokkaido prefecture had suspiciously said "Isn't it 'a local disease' in Hokkaido?", has now acquired its distinct disease entity worldwide [6]. To prevent children from suffering from this devastating disease condition, influenza vaccination must further be promoted. At the same time, development of more efficacious influenza vaccine is highly expected.

References

[1] Togashi T, Örvell C, Vartdal F, Norrby E. Production of antibodies against measles virions by use of the mouse hybridoma technique. Arch Virol 1981;67:149–57.

[2] Togashi T, Kuwajima S, Ozutsumi K, et al. Immunodiagnosis of measles giant cell pneumonia using mouse monoclonal antibodies against measles virus polypeptides. Nihon Shonika Gakkai Zasshi 1986;90:2294–300 [Japanese with English abstract].

[3] Togashi T, Matsuzono Y, Narita M. Epidemiology of influenza-associated encephalitis-encephalopathy in Hokkaido, the northernmost island of Japan. Pediatr Int 2000;42:192–6.

[4] Togashi T, Matsuzono Y, Morishima T, Narita M. Acute encephalitis-encephalopathy during influenza epidemics in Japanese children. Excerpta Med Int Congr Ser 2001;1219:609–13.

[5] Togashi T, Matsuzono Y, Narita M, Morishima T. Influenza-associated acute encephalopathy in Japanese children in 1994–2002. Virus Res 2004;103:75–8.

[6] Bhat N, Wright JG, Broder KR, et al. Influenza-associated deaths among children in the United States, 2003–2004. N Engl J Med 2005;353:2559–67.

Protease and helicase domains are related to the temperature sensitivity of wild-type rubella viruses

Masafumi Sakata [a,1], Tetsuo Nakayama [b,*]

[a] Research Laboratory II of Research and Development Division, Kitasato Institute Research Center for Biologicals, Saitama, Japan
[b] Laboratory of Viral Infection I, Kitasato Institute for Life Sciences, 5-9-1 Shirokane, Minato-ku, Tokyo, Japan

ABSTRACT

Wild-type rubella viruses grow well at 39 °C (non-temperature sensitivity: non-ts), while vaccine strains do not (temperature sensitivity: ts). Histidine at position 1042 of the p150 region of the KRT vaccine strain was found to be responsible for ts, while wild-type viruses had tyrosine at position 1042 (Vaccine 27; 234–42, 2009). The point-mutated virus (Y1042H) based on the wild-type unexpectedly showed little reduction in growth at 39 °C. In this report, several recombinant viruses were characterized, and point-mutated Y1042H together with the p90 region of KRT significantly reduced virus growth, compared to the parental wild-type virus. There was one amino acid difference at position 1497 of the helicase domain in the p90 region. Double mutation involving both positions 1042 and 1497 markedly reduced virus growth at 39 °C, but single substitution at 1497 did not. The other vaccine strain (TO-336vac) was investigated, and serine at position 1159 of the protease domain in p150 was a crucial amino acid for ts and non-ts characteristics among four amino acid substitutions between TO-336vac and the wild-type. Our results suggest that protease and helicase domains in non-structural protein were consistent with ts phenotype, possibly related to the attenuation process of wild-type viruses.

© 2010 Elsevier Ltd. All rights reserved.

1. Introduction

Rubella virus (RV) is the sole member of the genus *Rubivirus* in the family *Togaviridae*. The RV genome is single-stranded, positive-sense RNA of approximately 10 kb. The genome encodes two open reading frames (ORFs). One ORF is located at the 5′ end, encoding two non-structural proteins (NSPs), p150 and p90, required for replicating genomic RNAs. The motifs of methyltransferase and protease are located in p150, and the domains of helicase and RNA-dependent RNA polymerase are in p90. Another ORF is located at the 3′ end, encoding three structural proteins (SPs), capsid, E1, and E2, for the virion components. There are three untranslated regions (UTRs) at the 5′ and 3′ ends, and junction UTR (J-UTR) between the two ORFs [1,2].

RV infection occurs mostly in infants and children. Patients with RV infection develop low-grade fever, malaise, maculopapular rash, arthralgia, and post-auricular lymphadenopahty. Although most patients recover within several days without sequela, infection in unimmunized women during the first trimester of pregnancy

causes severe fetal defects known as congenital rubella syndrome (CRS) or fetal death. The common defects of CRS are deafness, cataracts, cardiac disease, and neurological abnormalities [3–6]. For the control of rubella outbreaks and prevention of CRS, live attenuated vaccines were developed and have been used in many countries [6,7].

Four live attenuated rubella vaccine strains have been used in Japan. Although the attenuation process was found to differ for each strain with serial passages of the wild-type rubella viruses in different primary cells at 35 °C or lower [8], all Japanese rubella vaccine strains exhibited unique but common characteristics of temperature sensitivity (ts) [9]. While wild-type viruses showed approximately 1/10 infective titers at 39 °C in comparison with that observed at a permissive temperature of 35 or 37 °C, vaccine strains with the ts phenotype demonstrated lower virus growth at 39 °C with less than 1/1000 at 35 or 37 °C.

The complete genomic sequences were determined for both the KRT live attenuated rubella vaccine and the wild-type RVi/Matsue.JPN/68 strain isolated at the same time and in the same district as the progenitor wild-type of KRT [10]. In order to determine the region responsible for the ts of KRT, a series of recombinant and point-mutated viruses were generated by reverse genetics (RG) [11–16], and infection experiments with cultured cells were carried out. The p150 gene, especially the histidine at position 1042 (His[1042]), was determined to be responsible for the ts phenotype of

* Corresponding author. Tel.: +81 35791 6269; fax: +81 3 5791 6130.
  E-mail address: tetsuo-n@lisci.kitasato-u.ac.jp (T. Nakayama).
  [1] Present address: Department of Virology III, National Institute of Infectious Diseases, Tokyo, Japan.

the KRT strain [10]. Conversely, it was not confirmed whether the introduction of His[1042] into the wild-type viruses influenced the growth of these viruses at 39 °C.

The objective of the present study was to identify whether the substitution of His[1042] was necessary and sufficient for the phenotype change from non-ts to ts, possibly causing attenuation of the wild-type viruses. Mutated recombinant viruses were generated based on the wild-type, RVi/Matsue.JPN/68, with subsequent investigation of virus growth at 39 °C, compared to that at 35 °C. The substitutions of His at position 1042 together with Ile at position 1497 were required for the acquisition of the ts phenotype. Moreover, Ser at position 1159 of the other vaccine strain (TO-336vac) was identified to be a crucial amino acid for the ts phenotype. These two positions (1042 and 1159) were located in the protease domain of p150, and this region was believed to play a key role in the non-ts and ts phenotypes, possibly related to the attenuation process.

2. Materials and methods

2.1. Cells and viruses

Vero and RK13 cells were maintained in Eagle's minimum essential medium (MEM) (Sigma–Aldrich, MO, USA) supplemented with 5% fetal bovine serum (FBS), penicillin (100 U/ml), and streptomycin (100 U/ml). Recombinant and point-mutated viruses were generated by RG, as reported previously [10]. Constructed RVs were propagated and stocked after one or two passages in Vero cells. The KRT vaccine seed strain was supplied by the Kitasato Institute, Research Center for Biologicals, and wild-type RVi/Matsue.JPN/68 strain was from the National Institute of Infectious Diseases Japan.

### 2.2. Construction of infectious cDNA clones of recombinant and point-mutated viruses

The infectious cDNA clones of RVi/Matsue.JPN/68 and KRT vaccine strains were constructed in a previous study and designated as pRViM and pKRT [10]. pH1042Y having a substitution at position 1042 of RVi/Matsue.JPN/68 was generated based on the pKRT, and the one with reversion, pY1042H, was constructed based on the pRViM, as shown Fig. 1.

Two recombinant clones, pY1042H-KRT p90 and pY1042H-KRT SP, were constructed, using the restriction enzyme sites Bsm I (gp 3243) and Not I (gp 6623) for recombination of the p90 region, and Xmn I (gp 6514) and EcoR I (3'end) for recombination of the SP region, as shown in Fig. 2.

The point-mutated clone in the p90 region, pT1497I, based on pRViM was constructed by PCR amplification with the GeneTailor™ Site-Directed Mutagenesis System (Invitrogen, CA, USA), using a set of forward, 5'-CGAGCGCACCGGCAtCTTCGCCTGCAACC-3' (gp 4516–4543) and reverse, 5'-TGCCGGTGCGCTCGCCCTCGATGTCATAA-3' (gp 4501–4529), primers, with the mutation site indicated as a lowercase letter. The double-mutated cDNA clone, pY1042H-T1497I, was developed with replacement of the fragments after digestion with restriction enzyme sites Bsm I (gp 3243) and Bgl II (gp 5355). The substitution sites of these constructions are shown in Fig. 3.

Four point-mutated clones (pC501R, pH573Y, pN1159S, and pN1351D) were generated by introducing the substitutions of TO-336 vaccine strain into pRViM, using the GeneTailor™ Site-Directed Mutagenesis System (Invitogen). Four substitutions at each of these sites are shown in Fig. 4.

Along with the genome structure of RV, we generated eight recombinant infectious cDNA clones, designated as pRViM rec1-8, replacing each region from 5' UTR, p150, p90, J-UTR, C, E2, E1, to 3' UTR of the RVi/Matsue.JPN/68 with the respective KRT region
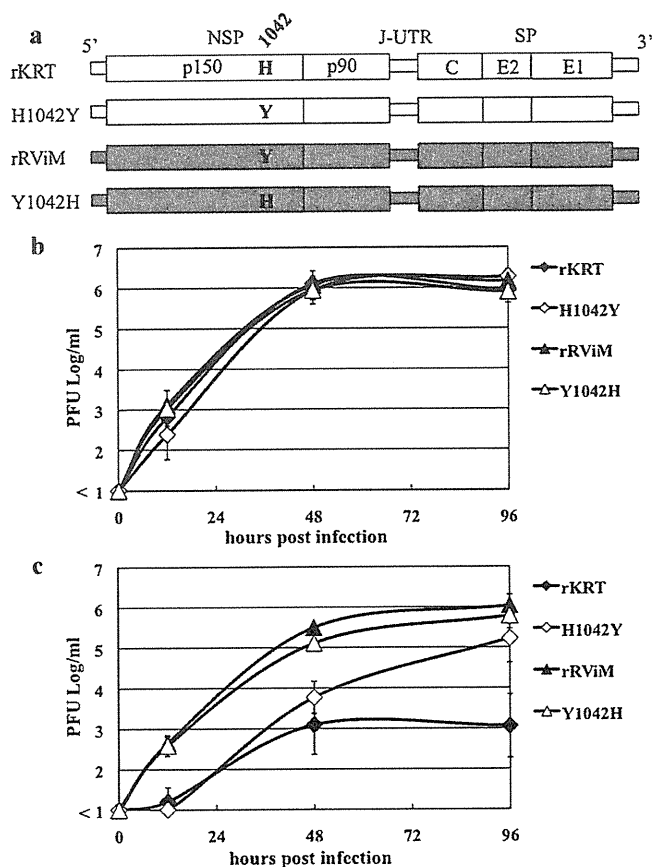

Fig. 1. The influence of the critical residue responsible for the ts of KRT on the growth of RVi/Matsue.JPN/68. (a) Construction of point-mutated viruses, H1042Y and Y1042H, based on rKRT and rRViM. The genomic structure of RV is indicated in the panel. The broad boxes demonstrate ORFs including NSP (p150 and p90) at the 5' end and SP (capsid, E2, and E1) at the 3' end. Narrow boxes outer than and between two ORFs show untranslated regions (5' UTR, J-UTR, and 3' UTR). H1042Y was constructed based on rKRT by introducing a substitution at position 1042 of rRViM. Y1042H was inversely constructed based on rRViM. The backbone based on rRViM is indicated as a gray bar, and open bars indicate the regions based on rKRT. (b) Growth kinetics of the point-mutated and parental viruses at 35 C. RK13 cells were infected at a MOI of 0.01. The culture medium was harvested at 12, 48, and 96 h post-infection (hpi), and the infective titer was measured by the plaque assay. The results show the average of three independent experiments and the error bar indicates ± standard deviation (S.D.) (c) Growth kinetics of the point-mutated and parental viruses at 39 C.

(Supplementary Fig. 1). A series of recombinant clones were constructed employing similar procedures to a previous report [10].

For the construction of the chimerical p150 region between pRViM and pKRT, seven recombinant viruses were constructed, introducing the complimentary region of pKRT into those of pRViM or pY1042H, using the restriction enzyme sites Mfe I (gp 126), Nde I (gp 1872), Nhe I (gp 2803), Bsm I (gp 3243), and EcoR V (gp 4213). These cDNA clones were named pRViM-KRT p150 rec 1, 2, 3, and 4, and pY1042H-KRT p150 rec 1, 2, and 4. pD1007G-Y1042H having the two substitutions of KRT was generated based on pY1042H instead of recombinant virus between Nhe I and Bsm I. The construction schemes are shown in Supplementary Figs. 2 and 3.

2.3. Recovery of clone viruses from infectious cDNA clones

Full-length viral genomic RNA was synthesized from the infectious cDNA clones with the mMESSAGE mMACHINE T7 kit (Applied Biosystems), following the instruction manual. Vero cells were cultured at 8.0×10^5 cells/well in 6-well plates 24 h before RNA transfection. After the cells were washed with 2.0 ml of OPTI-MEM,
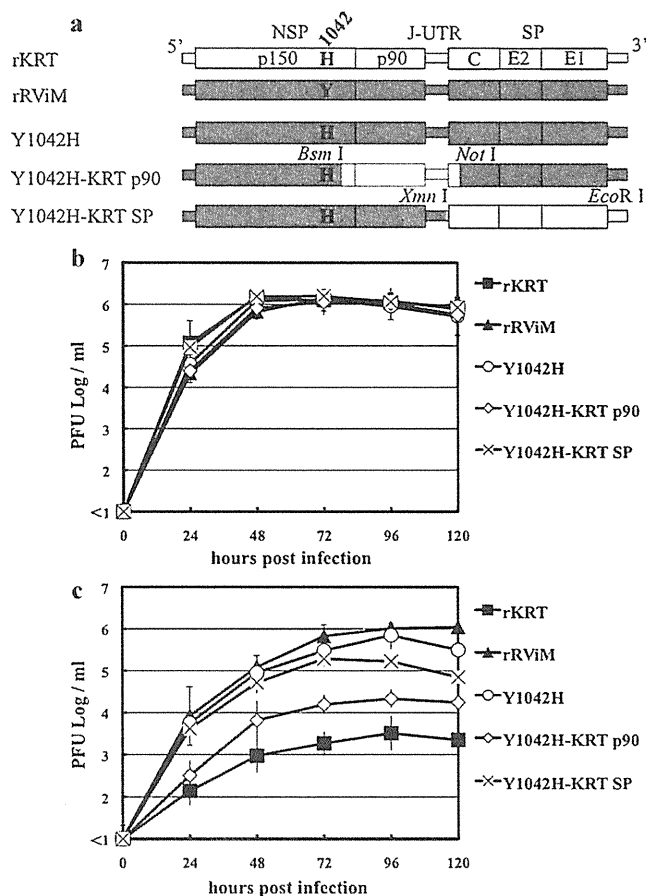
Fig. 2. Contributions of KRT genomic regions together with Y1042H on growth at 39 C.(a) Construction of recombinant viruses with Y1042H by replacing the p90 and SP of rRViM with those of rKRT. rKRT and rRViM were parental viruses, and Y1042H was the backbone virus for generating the recombinant viruses. Two recombinant viruses, Y1042H-KRT p90 and Y1042H-KRT SP, each having p90 and SP of KRT, were generated using the appropriate restriction enzyme sites (*Bsm* I, *Not* I, *Xmn* I, and *EcoR* I). The number in bold is the site of crucial for the *ts* phenotype of KRT. The gray bars represent those from rRViM and open bars are those from rKRT. (b) Growth kinetics of the recombinant viruses with Y1042H at 35 C. The culture medium was harvested every 24 h until 120 hpi. The titration of the medium was carried out using a plaque assay. The infective titer is shown as the average for three independent experiments and the error bar indicates ±S.D. (c) Growth kinetics of recombinant viruses at 39 C.
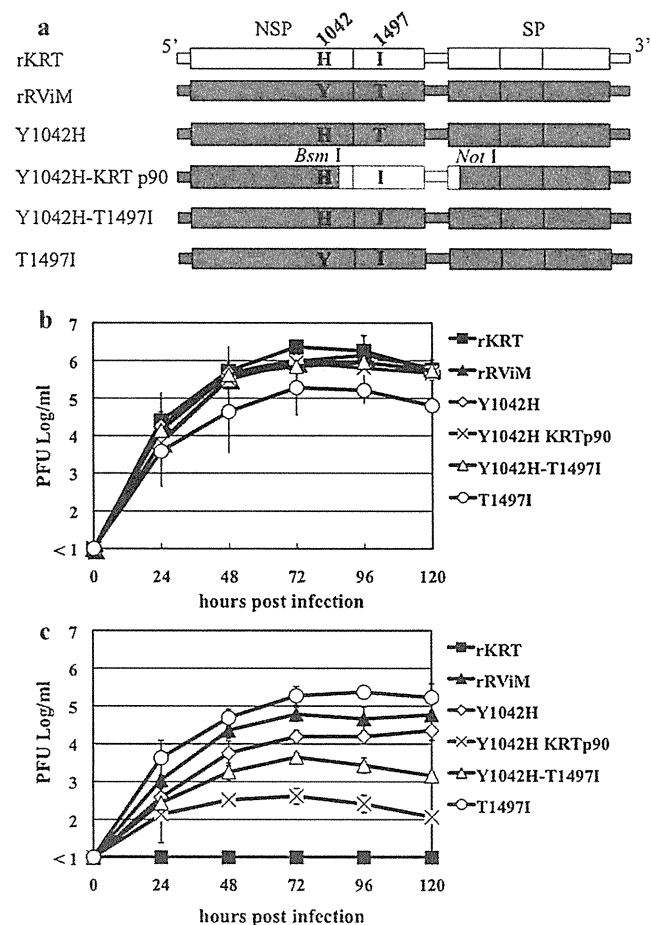
Fig. 3. Requirement of double mutations in p150 and p90 for the suppression of RVi/Matsue.JPN/68 growth at a high temperature. (a) Two point-mutated viruses, Y1042H-T1497I and T1497I, were constructed. The numbers in bold indicate sites where residues of wild-type viruses were replaced with those of KRT. Y1042H-T1497I was constructed based on Y1042H by replacing the threonine at position 1497 of RVi/Matsue.JPN/68 with the isoleucine of KRT. T1497I was generated by introducing the threonine at 1497 of KRT into rRViM. (b) Growth kinetics of the recombinant and mutated viruses at 35 C. The culture medium was harvested at 24, 48, 72, 96, and 120 hpi. The average infective titers in three independent experiments are shown and the error bar indicates ±S.D. (c) Growth kinetics of the recombinant and point-mutated viruses at 39 C.

RNA transfection was carried out with a mixture of 12.5 μg of synthesized RNA and 15.0 μl of DMRIE-C (Invitrogen) in 1.0 ml of OPTI-MEM. After incubation at 35 °C for 4 h, the mixture was removed and replaced with 2.0 ml of MEM containing 5% FBS. Culture media were harvested four days after transfection and stocked as master seed viruses.

2.4. Analysis of temperature sensitivity

Monolayers of RK13 cells in 6-well plates were infected at a multiplicity of infection (MOI) of 0.01. After adsorption, each well was washed twice with 2.0 ml of PBS and replaced with 2.0 ml of MEM containing 5% FBS and antibiotics. The plates were incubated at 35 or 39 °C in a 5% CO_2 incubator, and the culture medium was collected. The infective titer of the medium was determined based on the plaque assay.

2.5. Viral titration by plaque assay

Monolayers of RK13 cells in 6-well plates were infected with 100 μl of 10-fold serial dilutions of samples. The inoculum was

removed after contact for 1 h at room temperature and replaced with 3.0 ml of MEM containing 2% FBS, 40 μg/ml of DEAE dextran, 0.07% sodium bicarbonate, 0.7% agarose, penicillin at 100 U/ml, and streptomycin at 100 U/ml. The plates were incubated at 35 °C in a 5% CO_2 incubator. On day 7 post-infection, plaques were visualized by staining with PBS containing 0.1% crystal violet and 4% formalin [12,17,18].

2.6. Nucleotide sequence accession numbers

The accession number of the sequence and genotype used in this study for comparison are summarized in Table 1 [10,19–22].

3. Results

3.1. Influence of histidine at position 1042 on growth of wild-type virus at 39 °C

Our previous results showed that only the p150 region was responsible for the *ts* phenotype of a KRT vaccine strain among all genomic regions. Detailed analysis of four recombinant viruses in the p150 region was revealed that the region between *Nhe* I and
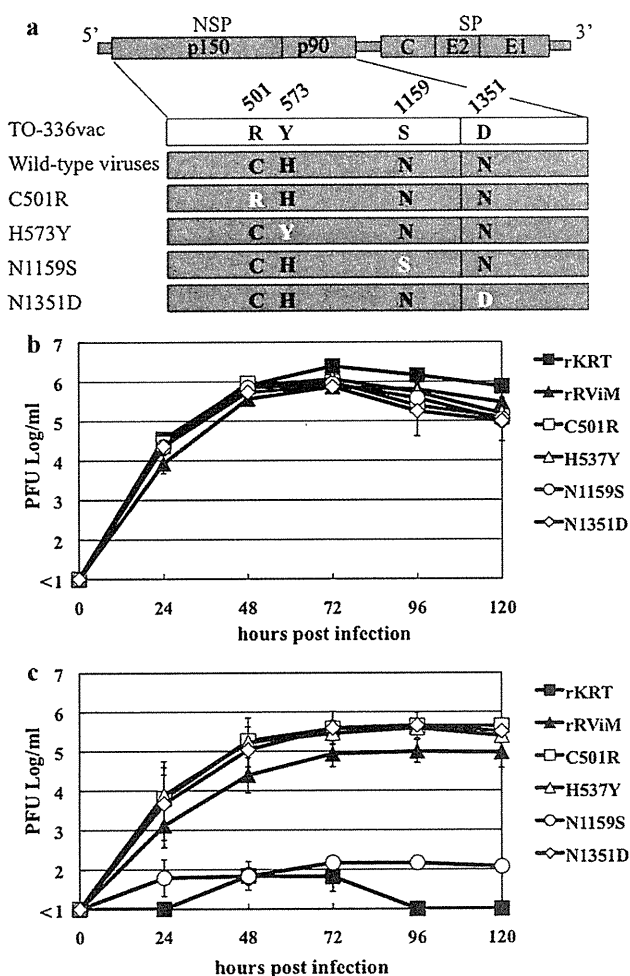
Fig. 4. Identification of crucial amino acid residues for the growth of wild-type viruses at 39 C based on TO-336vac. (a) Amino acid residues shown in the white bar represent unique residues in the NSP region of TO-336vac, and the gray bar indicates residues conserved among wild-type viruses. The numbers in bold show amino acid positions. White letters in gray bars represent the replacement of residues of wild-type viruses with those of TO-336vac. Four point-mutated viruses were generated based on rRViM. (b) Growth kinetics of the point-mutated viruses at 35 C. The infective titer is shown as the average of three independent experiments, and the error bar indicates ±S.D. (c) Growth kinetics of point-mutated viruses at 39 C.

Bsm I (genome position 2803–3243) was important for the ts of KRT and there were two amino acid substitutions at positions 1007 and 1042 (D and Y for RVi/Matsue.JPN/68, and G and H for KRT, respectively). Two residues of RVi/Matsue.JPN/68 were introduced into KRT solely or in combination to confirm the effect on the ts of KRT. The influence of aspartic acid residue at position 1007 on the ts was not observed, while tyrosine at position 1042 exerted a

strong effect on the ts. Thus, we concluded that histidine at position 1042 (His[1042]) was critical for the ts of KRT. However, it remained to be confirmed whether His[1042] is conversely crucial for growth of the wild-type virus at a restrictive temperature of 39 °C. For this reason, the present study was focused on the influence of residue at position1042 on the growth of wild-type virus at 39 °C. To assess the influence of His[1042] on the growth of wild-type viruses at 39 °C, we generated point-mutated viruses (Y1042H and H1042Y) based on pRViM and pKRT, respectively. RK13 cells were infected with the point-mutated viruses Y1042H and H1042Y, as well as parental viruses (rRViM and rKRT) at a moi of 0.01 and cultured at 35 and 39 °C. Culture media were harvested at 12, 48, and 96 hpi, and the results of virus growth are shown in Fig. 1. The growth kinetics of all viruses were the same at 35 °C, whereas the growth properties varied at 39 °C. rKRT with its ts phenotype exhibited a significant reduction in growth at 39 °C, with the peak titer of the virus infectivity at 39 °C being approximately 1/1000 of that at 35 °C. However, rRViM with its non-ts phenotype demonstrated virus growth at 39 °C similar to that at 35 °C, and the highest titer of the virus at 39 °C was about 1/5 of that at 35 °C. H1042Y also showed efficient growth at 39 °C, and the peak titer of the virus was 1/10 in comparison with that observed at 35 °C. These results were identical to our previous ones, but, unexpectedly, the peak titer of Y1042H at 39 °C did not decrease compared to that at 35 °C, and the growth kinetics of Y1042H at 39 °C were slightly lower than those of rRViM, with no significant differences.

3.2. Contribution of other genomic regions of KRT in combination with Y1042H to growth at 39 °C

The essential determinant of the ts phenotype of KRT was appeared to be histidine at position 1042, since the growth of H1042Y at 39 °C was markedly higher than that of KRT (Fig. 1). Moreover, it was observed that no genomic regions, except p150, contributed to the ts phenotype of KRT in our previous report [10]. Hence, we investigated whether the other region(s) participated in the growth of RVi/Matsue.JPN/68 at 39 °C in combination with His[1042]. Two recombinant viruses, Y1042H-KRT p90 and Y1042H-KRT SP, were generated employing a point-mutated virus based on rRViM with Y1042H. Y1042H-KRT p90 was constructed by exchanging the p90 region of RVi/Matsue.JPN/68 with that of KRT. Y1042H-KRT SP was generated by replacing the structural proteins (capsid, E2, and E1) of RVi/Matsue.JPN/68 with those of KRT. The growth kinetics of these viruses were examined at 35 and 39 °C (Fig. 2). There were no significant differences in the growth kinetics among the recombinant viruses (Y1042H, Y1042H-KRT p90, and Y1042H-KRT SP) and parental viruses (rKRT and rRViM) at 35 °C. At 39 °C, the growth kinetics of rRViM and Y1042H showed a very similar pattern, and there were no significant reductions in comparison with those at 35 °C. The replacement of the SP region of rRViM with that of KRT showed a small influence on the growth of

Table 1
Summary of genomic information on rubella viruses in this study.

Strain	Wild-type/vaccine	Clade	Genotype	GenBank accession no.
KRT	Vaccine	I	a	AB222608
TO-336vac	Vaccine	I	a	AB047329
RVi/Matsue.JPN/68	Wild-type	I	a	AB222609
RVi/TO-336wt.JPN/67	Wild-type	I	a	AB047330
RVi/SUR.SVK/74	Wild-type	I	a	AF435866
RVi/GUZ.GER/92	Wild-type	I	B	DQ388280
RVi/Anim.MEEX/97	Wild-type	I	C	DQ085341
RVi/JC2.NZL/91	Wild-type	I	D	DQ388281
RVi/6423.ITA/97	Wild-type	I	E	DQ085343
RVi/BRI.CN/79	Wild-type	II	A	AY258322
RVi/AN5.KOR/96	Wild-type	II	B	DQ085342
RVi/C4.RUS/67	Wild-type	II	c	DQ388279

rRViM at 39 °C, while that of the p90 region brought about a marked reduction in virus growth similar to that of rKRT at 39 °C. These results indicated that the non-*ts* phenotype of RVi/Matsue.JPN/68 altered the *ts* phenotype by the amino acid substitution of histidine at position 1042 together with the p90 region of KRT.

3.3. Determination based on KRT vaccine strain for wild-type viruses representing ts phenotype

There was a single amino acid difference at position 1497 in the p90 region between the two strains. The amino acid at position 1497 of p90 was changed from tyrosine (T) of RVi/Matsue.JPN/68 to isoleucine (I) of KRT. In order to decide on the amino acid residue responsible for altering the non-*ts* to *ts* phenotype, two mutated viruses, T1497I and Y1042H-T1497I, containing a single amino acid substitution at position 1497 or both at positions 1042 and 1497 of KRT were constructed, and the growth kinetics at 35 and 39 °C were investigated (Fig. 3). The growth kinetics of T1497I were slightly lower than those of the other viruses at 35 °C. They showed different patterns of growth at 39 °C. The maximum titer of rRViM and Y1042H at 39 °C was approximately 1/20 and 1/50 of those observed at 35 °C, respectively, and there was no significant change in the peak infective titer between the two. As for the growth kinetics of T1497I, there were no differences in the peak titer between 35 and 39 °C. The maximum titers of Y1042H-KRT p90 and Y1042H-T1497I at 39 °C were markedly lower than those at 35 °C. The peak titer of Y1042H-KRT p90 at 39 °C was less than 1/2000 of that at 35 °C. As for the amino acid difference in p90, the growth of Y1042H-T1497I clearly decreased, and the peak titer at 39 °C was approximately 1/200 of that at 35 °C. However, virus growth of Y1042H-T1497I at 39 °C was not identical to that of Y1042H-KRT p90.

To rule out any potential regions of KRT influencing virus growth of RVi/Matsue.JPN/68 at 39 °C, the effects of each genomic region of KRT were investigated on the growth of RVi/Matsue.JPN/68 at 39 °C, constructing a series of recombinant viruses (Supplementary Fig. 1). As in our previous study, there were no genomic regions except for the p150 region that reduced the growth of RVi/Matsue.JPN/68 at 39 °C. Replacement of the p90 region of pRViM with that of KRT did not alter the growth of RVi/Matsue.JPN/68 at 39 °C by itself. The effects of other fragments in the p150 region of KRT were investigated by generating a series of recombinant viruses (Supplementary Figs. 2 and 3). In the series of recombinant viruses based on pRViM and pY1042H, the kinetics of growth at 35 °C were very similar, and the peak titer at that temperature was approximately 10^6 PFU/ml. At 39 °C, the maximum titers of all recombinant viruses roughly exhibited a range of $10^{4.5-5}$ PFU/ml. Among those viruses, Y1042H and rRViM-KRT p150-rec 3, with His^{1042}, tended to show slightly weaker growth, and there were no regions that decreased the growth at 39 °C together with His^{1042}. Thus, the results strongly suggested that two mutations at positions 1042 and 1497 were essential for RVi/Matsue.JPN/68 representing the *ts* phenotype. The amino acid sequences of the NSP region were compared among KRT and wild-type viruses (Clade I: 1a, 1B, 1C, 1D, and 1E; Clade II: 2A, 2B, and 2c). Genomic information on those viruses is summarized in Table 1, and the characteristic amino acid residues of KRT that were otherwise conserved among wild-type viruses (Table 2). There were six amino acid differences in the NSP region, five residues in the p150 region, and one in the p90 region. Positions 295, 483, and 674 were located in a non-identified region, while those of 961, 1042, and 1497 were identified in X, protease, and helicase domains, respectively, which were highly conserved among wild-type viruses of all genotypes. These data conclusively demonstrated that two mutations at positions 1042 and 1497 were necessary for any wild-type viruses altering their non-*ts* phenotype to the *ts* of a KRT vaccine strain.

Table 2
Distinct amino acid residues in the NSP region of KRT that differed from wild-type viruses.

Position	Region	Domain	Amino acid differences	
			KRT	Wild-type viruses
295	p150	None	A	T
483	p150	None	A	T
674	p150	None	V	I
961	p150	X	V	A
1042	p150	Protease	H	Y
1497	p90	Helicase	I	T

Table 3
Unique amino acid residues in the NSP region of TO-336vac that differed from wild-type viruses.

Position	Region	Domain	Amino acid differences	
			TO-336vac[a]	Wild-type viruses
501	p150	None	R	C
573	p150	None	Y	H
1159	p150	Protease	S	N
1351	p90	Helicase	D	N

[a] The genomic sequence of TO-336 vaccine strain was cited from reference [19].

3.4. Other mutations in attenuation process of TO-336

It was hypothesized that the characteristic residue(s) for the *ts* phenotype of other vaccine strains would be located in NSP, especially protease and helicase domains, responsible for the growth of wild-type viruses at a high temperature. The TO-336 vaccine strain (TO-336vac) was investigated because all Japanese vaccine strains had the *ts* phenotype and the complete genomic sequences of TO-336vac and its parental wild-type virus (RVi/TO-336wt.JPN/67) were identified [19]. A comparison of the amino acid residues in NSP between TO-336vac and wild-type viruses is shown in Table 3. There were four substitutions at positions 501, 573, 1159, and 1351, and two residues at positions 1159 and 1351 were located in the protease and helicase domains, respectively. Each residue was introduced into pRViM, and the influence on growth at 39 °C is shown in Fig. 4. At 35 °C, the growth patterns of all viruses were similar and their peak titers were approximately 10^6 PFU/ml at 72 hpi. As for the growth at 39 °C, C501R, H537Y, and N1351D grew well and the peak titers of these viruses were approximately 4-hold higher than that of rRViM. On the other hand, the growth of N1159S was extremely poor at 39 °C, as well as that of rKRT. These results clearly demonstrated that serine at position 1159 was the critical determinant of a significant reduction in the growth of wild-type viruses at 39 °C, and it was responsible for the *ts* phenotype of the TO-336 vaccine strain.

4. Discussion

Vaccine strains have several biological differences such as cell tropism, plaque morphology, the *ts* phenotype, and immunogenic markers of rabbits and guinea pigs in comparison with wild-type viruses [8–11,13,23,24]. All rubella vaccine strains, RA27/3, KRT, TO-336vac, Matsuura, and Matsuba, which are available on the market, have the common feature of temperature sensitivity (*ts*). The *ts* phenotype is invaluable for analysis of the attenuation mechanisms of rubella viruses at the molecular level, because rubella vaccines were established through cold adaptation whereby isolated rubella wild-type viruses were serially passaged with human diploid or primary animal cells at 35 °C or less [8,25]. The acquisition of the *ts* phenotype during cold adaption was strongly correlated with the attenuation of their progenitor wild-type viruses, although the molecular mechanisms or

essential residues of the *ts* phenotype differ in each vaccine strain [10,19,26].

Through our previous experiments using the KRT vaccine strain, the genomic region responsible for the *ts* phenotype of the vaccine was identified using RG. The introduction of tyrosine at position 1042 of the RVi/Matsue.JPN/68 into rKRT resulted in growth recovery at 39 °C, and the rate of restoration was 100-fold higher than that of KRT. From these observations, a marked reduction was expected in the growth of RVi/Matsue.JPN/68 at 39 °C by introducing histidine at position 1042 (His^{1042}) into rRViM. However, this did not influence virus growth at 39 °C, and the growth kinetics of Y1042H at 39 °C barely reduced. Nevertheless, this result did not lessen the importance of our previous findings of the necessity of histidine at position 1042 for the *ts* of KRT, because H1042Y based on rKRT showed efficient growth at 39 °C in the present study (Fig. 1). These results suggested the possibility of additional modification at position 1042. The propensities of Y1042H-KRT p90 and Y1042H-T1497I at 39 °C were comparable, showing a significant reduction in virus growth compared to parental rRViM and Y1042H. Nonetheless, their growth patterns did not entirely coincide with that of rKRT (Figs. 2 and 3). This may be due to the differences in the genetic background between KRT and RVi/Matsue.JPN/68, because the growth properties at 39 °C showed diverse patterns in wild-type viruses and vaccine strains [24]. In fact, there was only one difference at the amino acid level in the p90 region between the two, but there were 65 differences at the nucleotide level. These nucleotide differences occurred through cold adaptation; thus, the accumulation of these mutations may be beneficial to replicate genomic RNAs at a low temperature, with the loss of stability of the genomic structure and efficiency of genomic replication at a high temperature. Alternatively, it remains a possibility that there is compatibility of conformational interaction between the viral genome and NSP. Consequently, the individual impacts of the p90 region and isoleucine at position 1497 of KRT on the growth of rRViM at 39 °C were not specifically identified (rRViM-rec3 in Supplementary Fig. 3 and T1497I in Fig. 3), and the influence of the mutation at 1497 on the growth at the temperature was exerted together with histidine at position 1042 with certainty. It is especially noteworthy that the combination of the two substitutions, at positions 1042 and 1497, with brought about more than a 100-fold reduction in growth at 39 °C compared with the parental rRViM.

Histidine at position 1042 and isoleucine at position 1497 were essential for altering the non-*ts* phenotype of any wild-type viruses with different genotypes to the *ts* phenotype, since those positions of wild-type viruses were highly conserved. These two amino acids were unique for the KRT strain. Next, the region(s) was investigated that was responsible for the *ts* of other vaccines. The TO-336 Japanese vaccine strain (TO-336vac) had four amino acid substitutions compared to wild-type viruses and each mutation was introduced into rRViM. A point-mutated virus (N1159S) was generated by introducing the serine at position 1159 of TO-336vac into rRViM, which exhibited a very similar pattern of growth at 39 °C to that of rKRT (Fig. 4). Interestingly, the effect of the single residue on virus growth of TO-336vac was more efficacious than the combination of two residues of KRT, and position 1159 was also located in the protease domain.

In our advanced study, the molecular function of the residue at position 1042 (H1042Y and Y1042H) was investigated regarding the steps of viral life cycles. Through the results of analysis concerning the efficiency of genomic replication, expression level of viral proteins in infected cells, and production of infective viruses in culture medium, the poor virus growth of the *ts* phenotype of KRT was due to the reduction of viral RNA synthesis, and RNA replication of the H1042Y at 39 °C was restored at a significant level (data not shown). On the other hand, Y1042H showed a declined genomic replication at 39 °C in comparison to that of rRViM; however, the

infective titer in the medium barely decreased. The efficacy of genomic replication was evidently affected by the substitution at position 1042. In the genomic replication of rubella virus, the non-cleaved NSP (p200) is essential for synthesizing the complementary genomic RNA (cRNA) as the template of viral genomic RNA (vRNA), while the cleavage complex of p150 and p90 is required for the efficient production of new vRNA as the template of synthesized cRNA. The replication stage of genomic RNA for both vRNA and cRNA is temporally controlled by the regulation of NSP processing [27]. Thus, the substitutions at position 1042 or 1159 would be correlated with the reduction in protease activity to cleave p200 into p150 and p90 and/or in the conformational stability of non-processed and processed NSP to limit viral RNA replication in each phase at a high temperature.

In other members of the family *Togaviridae*, Sindbis and Semliki Forest viruses, many *ts* mutants have a single mutation responsible for the *ts* phenotype in the protease or helicase domains, not combinations [28–33]. The *ts* phenotype represented by the combination of two mutations in protease and helicase domains may be characteristic of rubella virus. Interestingly, the protease domain of hepatitis C viral NS3 accelerated NS3 helicase activity, just as the helicase activity enhanced protease activity [34–36]. Protease and helicase domains of hepatitis C virus were located on one molecule of NS3, while the two domains of rubella virus locate on p150 and p90. These observations provide insights into structural and biochemical interactions. To account for the differences between H1042Y and Y1042H in *ts* or non-*ts* characteristics, the analysis of T1497I, Y1042H-T1497I, their inversion constructions in the viral life cycle, and biochemical characterization of the protease and helicase domains are currently under investigation.

In conclusion, using two vaccine strains, KRT and TO-336, we found that the mutations in the protease and helicase domains are necessary for the conversion of non-*ts* of wild-type viruses to the *ts* phenotype of vaccine strains. This may be applied to the other vaccine strains (RA27/3, Matsuura, and Matsuba) through further investigations.

Acknowledgment

Appendix A. Supplementary data

Supplementary data associated with this article can be found, in the online version, at doi:10.1016/j.vaccine.2010.11.074.

References

[1] Frey TK. Molecular biology of rubella virus. Adv Virus Res 1994;44:69–160.
[2] Chantler J, Wolinsky JS, Tingle A. Rubella virus. In: Knipe DM, Howley PM, editors. Fields virology. 4th ed. Philadelphia, PA: Lippincott Williams & Wilkins; 2001. p. 963–90.
[3] WHO. Rubella vaccines. WHO position paperWkly Epidemiol Rec; 2000.
[4] Plotkin SA. Rubella eradication. Vaccine 2001;19(May (25–26)):3311–9.
[5] Banatvala JE, Brown DW. Rubella. Lancet 2004;363(April (9415)):1127–37.
[6] Plotkin SA, Reef SE. In: Plotkin SA, Orenstein WA, editors. Vaccines. 4th ed. Philadelphia, PA: Elsevier Inc.; 2004. p. 707–43.
[7] Robertson SE, Featherstone DA, Gacic-Dobo M, Hersh BS. Rubella and congenital rubella syndrome: global update. Rev Panam Salud Publica 2003 Nov;14(5):306–15.
[8] Shishido A, Ohtawara M. Development of attenuated rubella virus vaccines in Japan. Jpn J Med Sci Biol 1976 Oct;29(5):227–53.
[9] Ohtawara M, Kobune F, Umino Y, Sugiura A. Inability of Japanese rubella vaccines to induce antibody response in rabbits is due to growth restriction at 39 degrees C. Arch Virol 1985;83(3–4):217–27.
[10] Sakata M, Komase K, Nakayama T. Histidine at position 1042 of the p150 region of a KRT live attenuated rubella vaccine strain is responsible for the temperature sensitivity. Vaccine 2009 Jan 7;27(2):234–42.

[11] Lund KD, Chantler JK. Mapping of genetic determinants of rubella virus associated with growth in joint tissue. J Virol 2000;74(January (2)):796–804.

[12] Pugachev KV, Abernathy ES, Frey TK. Improvement of the specific infectivity of the rubella virus (RUB) infectious clone: determinants of cytopathogenicity induced by RUB map to the nonstructural proteins. J Virol 1997;71(January (1)):562–8.

[13] Pugachev KV, Galinski MS, Frey TK. Infectious cDNA clone of the RA27/3 vaccine strain of Rubella virus. Virology 2000;273(July (1)):189–97.

[14] Tzeng WP, Frey TK. Complementation of a deletion in the rubella virus p150 nonstructural protein by the viral capsid protein. J Virol 2003;77(September (17)):9502–10.

[15] Wang CY, Dominguez G, Frey TK. Construction of rubella virus genome-length cDNA clones and synthesis of infectious RNA transcripts. J Virol 1994;68(June (6)):3550–7.

[16] Yao J, Gillam S. Mutational analysis, using a full-length rubella virus cDNA clone, of rubella virus E1 transmembrane and cytoplasmic domains required for virus release. J Virol 1999;73(June (6)):4622–30.

[17] Fogel A, Plotkin SA. Markers of rubella virus strains in RK13 cell culture. J Virol 1969;3(February (2)):157–63.

[18] Umino Y. Improved potency assay of rubella vaccine: parameters for plaque formation. J Virol Methods 1995;51(February (2–3)):317–28.

[19] Kakizawa J, Nitta Y, Yamashita T, Ushijima H, Katow S. Mutations of rubella virus vaccine TO-336 strain occurred in the attenuation process of wild progenitor virus. Vaccine 2001;19(April (20–22)):2793–802.

[20] Zheng DP, Zhou YM, Zhao K, Han YR, Frey TK. Characterization of genotype II Rubella virus strains. Arch Virol 2003;148(September (9)):1835–50.

[21] Zhou Y, Ushijima H, Frey TK. Genomic analysis of diverse rubella virus genotypes. J Gen Virol 2007;88(March (Pt 3)):932–41.

[22] Hofmann J, Renz M, Meyer S, von Haeseler A, Liebert UG. Phylogenetic analysis of rubella virus including new genotype I isolates. Virus Res 2003;96(October (1–2)):123–8.

[23] Linnemann Jr CC, Hutchinson L, Rotte TC, Hegg ME, Schiff GM. Stability of the rabbit immunogenic marker of RA 27-3 rubella vaccine virus after human passage. Infect Immun 1974;9(March (3)):547–9.

[24] Chantler JK, Lund KD, Miki NP, Berkowitz CA, Tai G. Characterization of rubella virus strain differences associated with attenuation. Intervirology 1993;36(4):225–36.

[25] Plotkin SA, Farquhar J, Katz M, Ingalls TH. A new attenuated rubella virus grown in human fibroblasts: evidence for reduced nasopharyngeal excretion. Am J Epidemiol 1967;86(September (2)):468–77.

[26] Pugachev KV, Abernathy ES, Frey TK. Genomic sequence of the RA27/3 vaccine strain of rubella virus. Arch Virol 1997;142(6):1165–80.

[27] Liang Y, Gillam S. Rubella virus RNA replication is cis-preferential and synthesis of negative- and positive-strand RNAs is regulated by the processing of nonstructural protein. Virology 2001;282(April (2)):307–19.

[28] Hahn YS, Strauss EG, Strauss JH, Rice CM, Levis R, Huang HV. Mapping of RNA- temperature-sensitive mutants of Sindbis virus: assignment of complementation groups A, B, and G to nonstructural proteins. J Virol 1989;63(July (7)):3142–50.

[29] De I, Sawicki SG, Sawicki DL. Sindbis virus RNA-negative mutants that fail to convert from minus-strand to plus-strand synthesis: role of the nsP2 protein. J Virol 1996;70(May (5)):2706–19.

[30] Suopanki J, Sawicki DL, Sawicki SG, Kaariainen L. Regulation of alphavirus 26S mRNA transcription by replicase component nsP2. J Gen Virol 1998;79(February (Pt 2)):309–19.

[31] Lulla V, Merits A, Sarin P, Kaariainen L, Keranen S, Ahola T. Identification of mutations causing temperature-sensitive defects in Semliki Forest virus RNA synthesis. J Virol 2006;80(March (6)):3108–11.

[32] Balistreri G, Caldentey J, Kaariainen L, Ahola T. Enzymatic defects of the nsP2 proteins of Semliki Forest virus temperature-sensitive mutants. J Virol 2007;81(March (6)):2849–60.

[33] Rice CM, Levis R, Strauss JH, Huang HV. Production of infectious RNA transcripts from Sindbis virus cDNA clones: mapping of lethal mutations, rescue of a temperature-sensitive marker, and in vitro mutagenesis to generate defined mutants. J Virol 1987;61(December (12)):3809–19.

[34] Beran RK, Serebrov V, Pyle AM. The serine protease domain of hepatitis C viral NS3 activates RNA helicase activity by promoting the binding of RNA substrate. J Biol Chem 2007;282(November (48)):34913–20.

[35] Beran RK, Pyle AM, Hepatitis. C viral NS3-4A protease activity is enhanced by the NS3 helicase. J Biol Chem 2008;283(October (44)):29929–37.

[36] Rajagopal V, Gurjar M, Levin MK, Patel SS. The protease domain increases the translocation stepping efficiency of the hepatitis C virus NS3-4A helicase. J Biol Chem 2010;285(June (23)):17821–32.
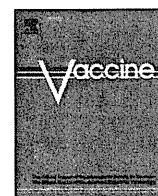
AIK-C measles vaccine expressing fusion protein of respiratory syncytial virus induces protective antibodies in cotton rats

Akihito Sawada[a], Katsuhiro Komase[b], Tetsuo Nakayama[a,*]

[a] Laboratory of Viral Infection I, Kitasato Institute for Life Sciences, Kitasato University, Shirokane 5-9-1, Minato-ku, Tokyo 108-8641, Japan
[b] Department of Virology III, National Institute of Infectious Diseases, Musashimurayama, Tokyo 208-0011, Japan

ABSTRACT

Respiratory syncytial virus (RSV) is the most common cause of respiratory infection in infants, and no vaccine is available. In this report, recombinant AIK-C measles vaccines, expressing the RSV G or F protein of subgroup A (MVAIK/RSV/G or F), were investigated as a RSV vaccine candidate. MVAIK/RSV/G or F had the original ts phenotype and expressed RSV/G or F protein. Cross-reactive neutralizing antibodies against RSV subgroups A and B were detected in cotton rats immunized intramuscularly with MVAIK/RSV/F but not MVAIK/RSV/G. In cotton rats infected with RSV, RSV was recovered and lung histopathological finding was compatible with interstitial pneumonia, demonstrating thickening of alveolar walls and infiltration of mononuclear cells. When cotton rats immunized with MVAIK/RSV/F were challenged with homologous RSV subgroup A, no infectious RSV was recovered and very mild inflammation was noted without RSV antigen expression. When they were challenged with subgroup B, protective efficacy decreased. When cotton rats immunized with MVAIK/RSV/G were challenged with RSV subgroup A, low levels of infectious virus were recovered from lung. When challenged with subgroup B, no protective effects was demonstrated, demonstrating large amounts of RSV antigen in bronchial-epithelial cells. MVAIK/RSV/F is promising candidate and protective effects should be confirmed in monkey model.

© 2010 Elsevier Ltd. All rights reserved.

1. Introduction

Human respiratory syncytial virus (RSV) is a member of the family Paramyxoviridae in the order Mononegavirales. The Paramyxoviridae consist of two subfamilies, Paramyxovirinae and Pneumovirinae [1]. Classified into the genus Pneumovirus, RSV is characterized by a non-segmented, negative sense, single-stranded RNA genome, and has approximately 15,200 nucleotides. All members of the paramyxovirus family are similar in structure and characteristics [2]. Viral particles of RSV are surrounded by a lipid bilayer with two viral glycoproteins, G and F [1], involved in the attachment to, fusion with, and entry into cells during infection. G protein is not always required for infection and cell fusion and the expression of F protein alone leads to cell fusion [3]. RSV was first isolated in 1956 and two antigenically different subgroups, A and B, co-circulate [4]. RSV is the most common cause of lower respiratory infections in infants and young children worldwide, and is responsible for a variety of illnesses, including 20–25% of pneumonia cases and 45–50% of bronchiolitis cases among hospitalized children [5]. The peak of serious RSV infections is at 2–6 months of age and most children experience an RSV infection by two years of

age [6]. The infection causes serious illnesses especially in babies born prematurely and having chronic lung diseases, or congenital heart diseases. RSV also causes lower respiratory tract infections in the elderly, and in immunocompromised hosts [7]. The global annual morbidity and mortality for RSV are estimated to be 64 million and 160,000 deaths, respectively [8].

A recent study of the immune response to RSV showed the importance of innate immunity in regulating adaptive immune responses [9]. Adaptive immunity is generally considered effective due to neutralizing antibodies (NT) and cellular immune responses for the clearance of viruses are influenced by innate inflammatory responses. Secretory and NT antibodies were generated after repeated infections with RSV, although the responses were weak in young infants [10]. The presence of IgG antibodies in the lung has been shown to reduce viral load [11]. Even a natural infection did not provide long-term protective immunity against reinfection in young infants, and a humanized monoclonal antibody against the F protein is available as a prophylaxis against RSV, or for reducing serious diseases in high-risk infants during epidemics [12]. However, the high medical costs for monthly administration mean that there is a great need to develop an RSV vaccine [13]. There are several obstacles to developing a RSV vaccine. An aluminium-precipitated formalin-inactivated RSV vaccine (FI-RSV) was developed in the 1960's, but did not prevent infections [14]. In fact, symptoms were exacerbated among recipients subsequently

infected with RSV. FI-RSV generated only binding antibodies without neutralizing activity because of the denatured F protein, and did not induce cytotoxic T cell lymphocytes (CTL) activity [15]. Several strategies have been adopted to develop subunit vaccines, live attenuated vaccines through conventional methods of cloning or selecting *ts* mutants, genetically modified-strain by reverse genetics, and vaccinia virus vector-based recombinant vaccines [16–18].

Recently, a method for direct manipulation of the genomic RNA of *Mononegavirales* has been established, known as the infectious cDNA clone system [19]. The transcription and replication of minigenome RNA are driven by viral proteins, which are co-expressed by plasmids or helper viruses. Using this system, the infectious recombinant viruses can be retrieved from the authentic full-size genome cDNA [20,21]. These "reverse genetics" techniques are powerful tools not only for basic research into viral properties, such as the characteristics of viral proteins, and mechanisms of replication, transcription and pathogenesis, but also for practical purposes, such as the development of new vaccines and viral vectors. As vector-based recombinant vaccines, human parainfluenza virus type III (HPIV III) vector-based, or Sendai virus vector-based vaccines have been evaluated [22,23].

Current measles vaccines used throughout the world were attenuated from the Edmonston strain, classified as genotype A [24]. The AIK-C strain of the measles vaccine was developed in 1976 in Japan from the Edmonston strain, by plaque cloning through passages in sheep kidney cells and chicken embryonic cells at 33 °C [25]. It shows optimal growth at 33 °C and little or no growth at 39 °C [21]. The safety and immunogenicity of the AIK-C measles vaccine were established through clinical trials [26–29]. Reverse genetics of the AIK-C live attenuated vaccine was performed and in this study, recombinant AIK-C MV vaccine strains encoding the RSV G or F protein were constructed, and immunogenicity and protective effects against RSV were investigated in cotton rats immunized with recombinant measles vaccines, expressing RSV G or F protein.

2. Materials and methods

2.1. Viral strains and cell cultures

The AIK-C seed strain for vaccine production was used. Wild-type strains of RSV subgroups A and B were isolated in HEp-2 cells from patients. Long and wild-type strains were used for the neutralization test (NT) against RSV subgroups A and B. 293T and HEp-2 cells were maintained in Eagle's MEM (Sigma–Aldrich, Dorset, UK) supplemented with 10% fetal bovine serum (FBS). Vero cells were maintained in Eagle's MEM supplemented with 5% FBS. B95a cells are marmoset B cell line, and maintained in RPMI-1640 medium (Sigma–Aldrich, Dorset, UK) supplemented with 10% FBS [30]. These media were supplemented with 4 mM L-glutamine, 10,000 IU/ml penicillin, and 10,000 μg/ml streptomycin.

2.2. Cloning of the RSV G and F genes

Genomic RNA was extracted from a clinical isolate of subgroup A and B, and the RSV genome was amplified by RT-PCR. The viral RNA was first converted to cDNA using a cDNA primer: 5'-ACACGATTTGCAATCAAACC-3'. The RSV G gene was amplified with 5'-GTTTCCATGGCCAAAACCAAGGACCAA-3' and 5'-CCAAGCGGCCGCTAGTTTGTTGTGTTGGATGGAGA-3', which amplified 894 bp. The RSV F gene was amplified with 5'-GTTGCCATGGAGTTGCCAATCCTCAA-3' and 5'-TGTGGCGGCCGCTAACTAAATGCAATATTATTT-3', which amplified 1722 bp. The F and G genes were cloned into pMV/20-77 using two restriction enzymes, Nco I and Not I (underlined sequences).

2.3. Construction of recombinant AIK-C

A schematic diagram of the strategy used for the construction of the recombinant cDNA plasmid is shown in Fig. 1. The full length plasmid was divided from two parts as previously reported. The first half contained the N, P, M and F genes from the leader sequence to the Pac I site at nucleotide position 7238 of the AIK-C genome. The second half contained the H and L regions from the Pac I site from position 7238 of the AIK-C genome to the trailer sequence. The full-length cDNA, pMVAIK, was constructed using these two plasmids [31].

The cloning vector for the RSV genome, pMVAIK/20-77, was constructed from positions 2040 (Sac II) to 7761 (EcoT22 I). The RSV G or F PCR product was digested with Nco I and Not I and ligated into pMVAIK/20-77, resulting in pMVAIK/20-77/RSV/G and pMVAIK/20-77/RSV/F, respectively. The pMVAIK/20-77/RSV/G or pMVAIK/20-77/RSV/F was digested with Sac II and Pac I and ligated into pMVAIK. Then, full-length infectious cDNA clones, pMVAIK/RSV/G and pMVAIK/RSV/F, were constructed.

2.4. Rescue of the infectious recombinant virus from cloned cDNA

Monolayers of 293T cells in 6-well plates were infected with the vaccinia virus MVAT7 pol, expressing T7 RNA polymerase. MVAT7 pol was derived from a highly attenuated and host range-restricted vaccinia virus, the Ankara strain [32]. Open reading frames of the N, P, and L genes were cloned downstream of the T7 promoter of pBluescript SK, and the expression plasmids pCIAN01, pCIAP01, and pCIAL01 were constructed [19,21]. After 1 h of adsorption, the cells were washed with Opti-MEM (GIBCO, Grand Island, NY, US) and transfected with 0.5 μg of pCIAN01, 0.25 μg of pCIAP01, 0.1 μg of pCIAL01, and 1.5 μg of pMVAIK/RSV with TransIT-LT1 Reagent (Mirus Bio Corporation, US). After incubation at 33 °C for 3 h, the medium containing the transfection reagent/plasmid complex was replaced with fresh MEM supplied with 5% FBS. The transfected cells were incubated at 33 °C in 5% CO$_2$ for 3 days. After 3 days, 293T cells were detached and co-cultured with B95a cells. When a demonstrable cytopathic effect (CPE) was observed, the supernatant and cell lysate were harvested and stocked.

2.5. Virus growth

To examine viral growth, B95a cells were infected with MVAIK, MVAIK/RSV/G, and MVAIK/RSV/F (m.o.i. = 0.02) and the plates were placed at temperatures of 33, 35, 37 and 39 °C. The culture fluids were obtained on days 1, 3, 5, and 7 of culture and infective titers were examined and expressed as TCID$_{50}$/ml in B95a cells.

2.6. Indirect immuno-staining and Western blotting

B95a cells were infected with MVAIK, MVAIK/RSV/G or MVAIK/RSV/F at m.o.i. of 0.01 in 24-well plates and cultured for two days at 33 °C. B95a cells were collected and subjected to indirect immuno-staining without fixation to detect the surface expression. Polyclonal antibodies against RSV raised in goat (Abcam, Cambridge, UK) were used and the cells incubated for 1 h at 37 °C. The cells were washed extensively with phosphate-buffered saline with 0.05% Tween 20 (PBST), and stained with second antibodies against goat IgG conjugated with FITC, raised in rabbit (Vector Laboratories, Burlingame, CA, US), and thereafter, mouse monoclonal antibody against MV HA protein (kindly supplied by Dr. Sato, National Institute of Infectious Diseases, Japan) was used and followed by second antibodies against mouse IgG conjugated with rhodamine raised in goat (Rockland Immunochemicals, Gilbertsville, PA, US).

Vero cells were infected with MVAIK, MVAIK/RSVF, and MVAIK/RSV/G and HEp-2 were infected with RSV subgroup A, Long
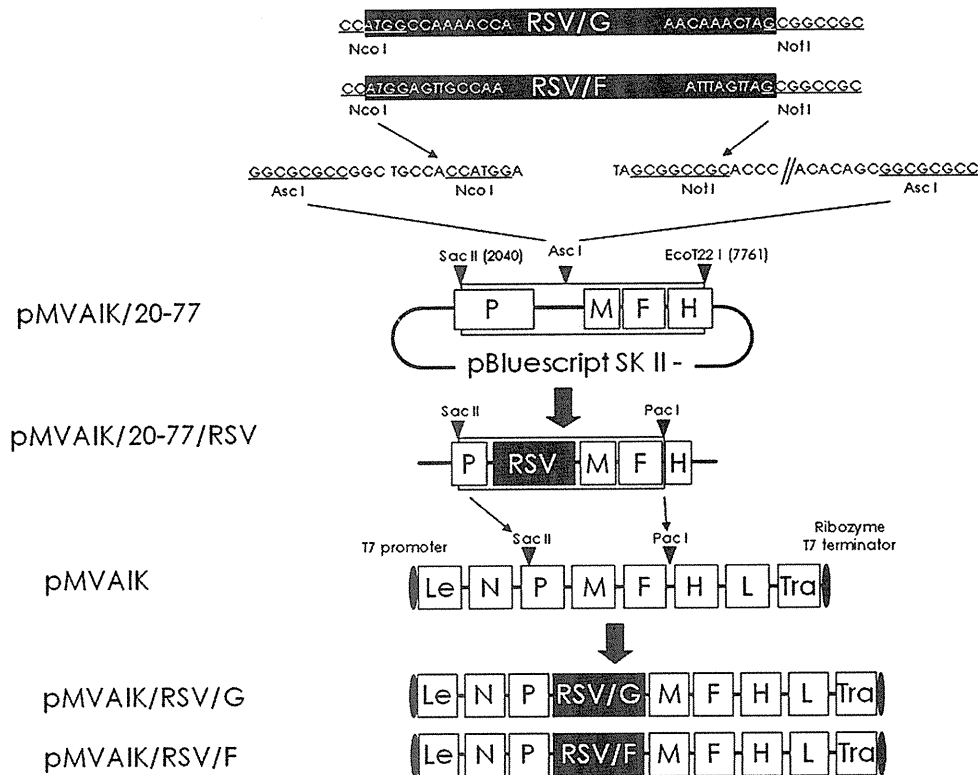
Fig. 1. Strategy for the construction of the recombinant AIK-C genome cDNAs having RSV protein genes. The recombinant AIK-C viral cDNAs expressing RSV G or F protein were constructed based on AIK-C cDNA (pMVAIK). pMVAIK/20-77 was constructed for the cloning of foreign genes. The Asc I site was introduced by adding GGCGCG after position 3432 of AIK-C and R1 and R2 sequences were added. The Nco I–Not I fragment of RSV G or F was cloned into pMVAIK/20-77, designed as pMVAIK/20-77/RSV. pMVAIK/20-77/RSV had unique restriction enzyme sites, Sac II and Pac I sites, located in the P gene and between the F and H gene. The DNA fragments between the Sac II and Pac I sites of pMVAIK/20-77/RSV/G and pMVAIK/20-77/RSV/F were inserted into pMVAIK using Sac II and Pac I sites. The recombinant plasmid constructs were designated pMVAIK/RSV/G and pMVAIK/RSV/F, respectively.

strain in a 24-well plate. Culture supernatants were collected and cells were freeze-thawed and total protein of 4 μg of supernatants and cell lysate was applied. Samples were subjected to Western blotting. Briefly, after SDS-PAGE, proteins were transferred to membrane (Immobilon; Millipore, Danvers, MA, US). Membranes were washed with PBST, incubated with an RSV polyclonal antibody raised in goats, washed again, and incubated with a donkey anti-goat IgG (H + L) conjugated with horse radish peroxidase (HRP). The final reaction was performed with a DAB SUBSTRATE KIT FOR PEROXIDASE (Vector Laboratories, Burlingame, CA, US) used as recommended by the manufacturer.

Culture medium of Vero cells infected with MVAIK/RSV/G or F was collected and fractionated through sucrose discontinuous gradient ultra-centrifugation. Fraction 1 was obtained at the top of the gradient, 30% sucrose, Fraction 2 between 30% and 45% sucrose, and Fraction 3 between 45% and 60% sucrose. Each fraction was electrophoresed and analyzed by Western blotting, using RSV polyclonal antibodies and monoclonal antibodies against MV N protein.

2.7. Immunogenicity in experimental animals

Six-week-old cotton rats were purchased from Harlan (Indianapolis, IN, US) and Charles River (USA). Five cotton rats for each group were immunized intramuscularly with $1 \times 10^6 \, TCID_{50}$ of MVAIK, MVAIK/RSV/G or MVAIK/RSV/F. Serum samples were obtained immediately before and 1, 3, 5, 8, 12 and 16 weeks after immunization. Cotton rats immunized with MVAIK/RSV/G or F were boosted with the same dose after 16 weeks, and serum samples were collected one week after re-immunization (17 weeks).

2.8. Serology

Neutralization tests (NTs) against RSV were performed with the 50% plaque reduction assay, using Long strain and wild-type isolate of subgroup B. Briefly, serum samples were serially diluted by1:4, starting from a 1:10 dilution, and mixed with an equal volume of RSV (100 PFU) in MEM for 1 h at room temperature. The mixtures were inoculated on monolayers of HEp-2 cells in 24-well plates. Plates were incubated for 1 h at 37 °C in 5% CO$_2$ and then overlaid with MEM supplemented with glutamine, antibiotics, 5% fetal bovine serum and 0.5% agar. After incubation for six days at 37 °C in 5% CO$_2$, cells were fixed with 1% formalin. Agar was removed and cells were stained with neutral red. Plaque numbers were counted and NT antibody titers were calculated as the reciprocal of the serum dilutions that showed a 50% reduction of the plaque number.

For the particles agglutination (PA) test, gelatin particles were coated with purified measles virus antigen (Serodia®-Measles, Fuji Rebio, Tokyo, Japan). Sera were serially diluted two-fold, starting from a 1:10 dilution, and each serum dilution was mixed with an equal volume of gelatin particles to detect agglutination, according to the recommendations of the manufacturer. The PA antibody titers were expressed as the reciprocal of the serum dilution which induced particle agglutination.

2.9. Detection of the MV genome

Cotton rats were sacrificed 10 days after immunization with MVAIK/RSV/G and F, and samples of liver, kidney, spleen, lung, thymus, and nasal turbinate were obtained to detect the MV genome. The tissues were homogenized, and total RNA was

Table 1
Primer and probe sequences for the detection of the MVAIK N gene and RSV N gene by TaqMan real-time PCR.

Primers	Sequences (5'–3')	Genomic position
RSV-Long-N-(+)	aatgctaaaagaaatgggagagg	
Probe	gctccaga	411–470
RSV-Long-N-(−)	ccacaatcaggagaatcatgc	
MV-AIK-C-N-(+)	caagatcagtagagcggttgg	
Probe	agcccaag	1212–1274
MV-AIK-C-N-(−)	ctttgatcaccgtgtagaaatga	

extracted using an RNeasy® Plus Mini Kit (QIAGEN, MD, US), as recommended. TaqMan PCR was performed in the MV N gene region. Reverse-transcribed real-time PCR was performed using a FastStart TaqMan® Probe Master (Roche Meylan, France), and LightCycler®480 System II (Roche Meylan, France) using 1 μg of extracted mRNA. cDNA was synthesized using an One Step PrimeScript® RT-PCR Kit (TaKaRa Bio, Otsu, Japan). The parameters used were 1 cycle of 95 °C for 10 min, 45 cycles of 95 °C for 10 s, 60 °C for 30 s, and 72 °C for 1 s, and 1 cycle of 40 °C for 30 s. Reactions were performed in triplicate and genome copy numbers were determined by referring to the results of serial dilution of the corresponding plasmid, pCIAN01. The primers used in TaqMan PCR are shown in Table 1.

2.10. Protection against RSV

Seven week-old cotton rats were immunized intramuscularly with MVAIK/RSV/F or MVAIK/RSV/G and, five weeks later, challenged with 10^6 PFU/0.5 ml of RSV subgroups A and B. They were sacrificed four days after the challenge and nasal wash, BAL, nasal turbinate, and lung tissues were obtained. Lung samples were divided into two portions, one for pathological examination, and another for recovering the infective particles and RSV genome.

Tissues were homogenized and 0.1 ml volumes of serial 10-fold dilutions of homogenized samples were placed on HEp-2 cells and overlaid with MEM 5% FBS and 0.5% agar. Plaque numbers were counted after incubation for six days at 37 °C and infectivity was expressed as the number of plaques. RNA was extracted from nasal wash, BAL, nasal turbinate and lung homogenate. cDNA was synthesized and reverse-transcribed real-time PCR was done at position 1212–1274 of the RSV N genome, using the primers and TaqMan probe listed in Table 1. The RSV genome copy number was calculated by referring to a linear regression assay of serial dilutions of the corresponding plasmid.

Lungs were inflated to their normal volumes with 4% formalin and submerged in formalin for overnight fixation. The fixed tissue was embedded in paraffin, sectioned, and stained with hematoxylin–eosin, and immuno-staining was performed using four clone blend monoclonal antibodies against RSV P, F, and N proteins (AdB Serotec, UK), and anti-mouse IgG conjugated with HRP.

3. Results

3.1. Characteristics of recombinant viruses

MVAIK/RSV/G and MVAIK/RSV/F were recovered from full-length recombinant cDNA and MVAIK from vector cDNA. B95a cells were infected with MVAIK, MVAIK/RSV/G and MVAIK/RSV/F at a m.o.i. of 0.02. The culture medium was harvested on days 1, 3, 5, and 7 at 33 °C and the results are shown in Fig. 2. Infectivity showed a peak titer of 10^5 TCID$_{50}$/ml 5 days after infection. MVAIK/RSV/G and MVAIK/RSV/F grew as well as MVAIK in B95a cells. AIK-C has temperature-sensitivity (ts), showing efficient virus
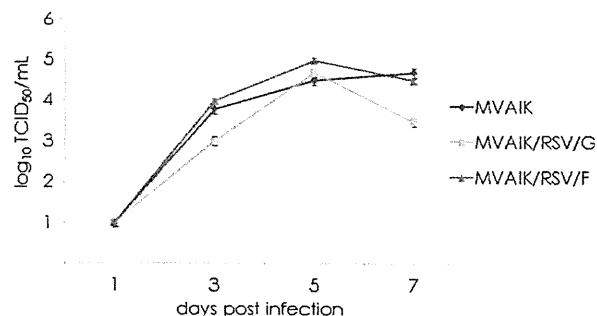
Fig. 2. Growth of MVAIK, MVAIK/RSV/G, and MVAIK/RSV/F. B95a cells were infected with MVAIK, MVAIK/RSV/G, and MVAIK/RSV/F at m.o.i. of 0.02. Culture fluid was obtained on days 1, 3, 5, and 7 of culture at 33 C. Infectivity is shown as mean titers of TCID$_{50}$/ml assayed in B95a cells. Error bars show 1.0 S.D.
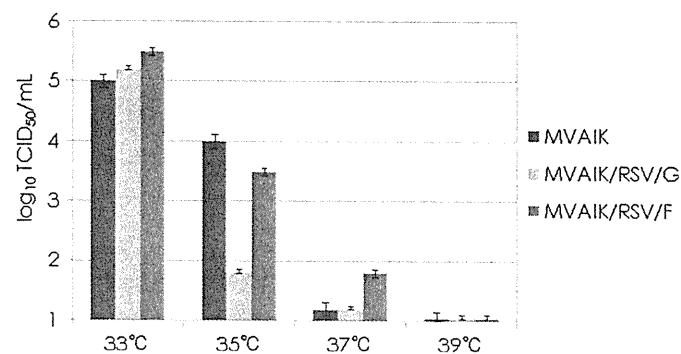
Fig. 3. Temperature sensitivity of MVAIK, MVAIK/RSV/G, and MVAIK/RSV/F. B95a cells were infected with MVAIK, MVAIK/RSV/G, and MVAIK/RSV/F at a m.o.i. of 0.02. Culture fluid was obtained on day 5 and the infectivity at 33 C, 35 C, 37 C, and 39 C is shown as mean infectious titer (TCID$_{50}$/ml). Error bars show 1.0 S.D.

growth at 33 °C, but extremely poor at 39 °C, less than 10^{-4} in comparison with the result at 33 °C. MVAIK/RSV/G and MVAIK/RSV/F were examined for virus growth at 33, 35, 37 and 39 °C. The culture supernatants were harvested on day 7 of the culture and infectivity was examined. Both MVAIK/RSV/G and MVAIK/RSV/F showed 10^5 TCID$_{50}$/ml at 33 °C, and MVAIK/RSV/F grew little at 37 °C. But, however, no infectious virus was detected at 39 °C, and the ts phenotype was maintained (Fig. 3).

3.2. Detection of RSV G or F protein

B95a cells were infected with MVAIK/RSV/F, MVAIK/RSV/G, and MVAIK at a m.o.i. of 0.01. Live cells were stained with monoclonal antibodies against measles HA and polyclonal antibodies against RSV and visualized with second antibodies conjugated with rhodamine or FITC, as shown in Fig. 4. RSV F and MV HA proteins were observed diffusely on the surface of B95a cells infected with MVAIK/RSV/F. RSV G protein was detected in speckled pattern together with MV HA protein on the surface of B95a cells infected with MVAIK/RSV/G.

Culture medium and cell lysate were examined for the expression of RSV G and F by Western blotting and the results are shown in Fig. 5. Live vector virus MVAIK and RSV were used for the negative and positive controls. RSV G and F proteins were detected in both supernatant and cell lysate infected with MVAIK/RSVF, and MVAIK/RSV/G, similar to those infected with RSV (Fig. 5, Panel A).

Culture fluid was collected and fractionated through sucrose discontinuous gradient ultra-centrifugation. Fraction 1 was obtained at the top of the gradient, 30% sucrose, Fraction 2 between 30% and 45% sucrose, and Fraction 3 between 45% and 60% sucrose. Each fraction was electrophoresed and analyzed by Western blotting, using RSV polyclonal antibodies and a monoclonal antibody
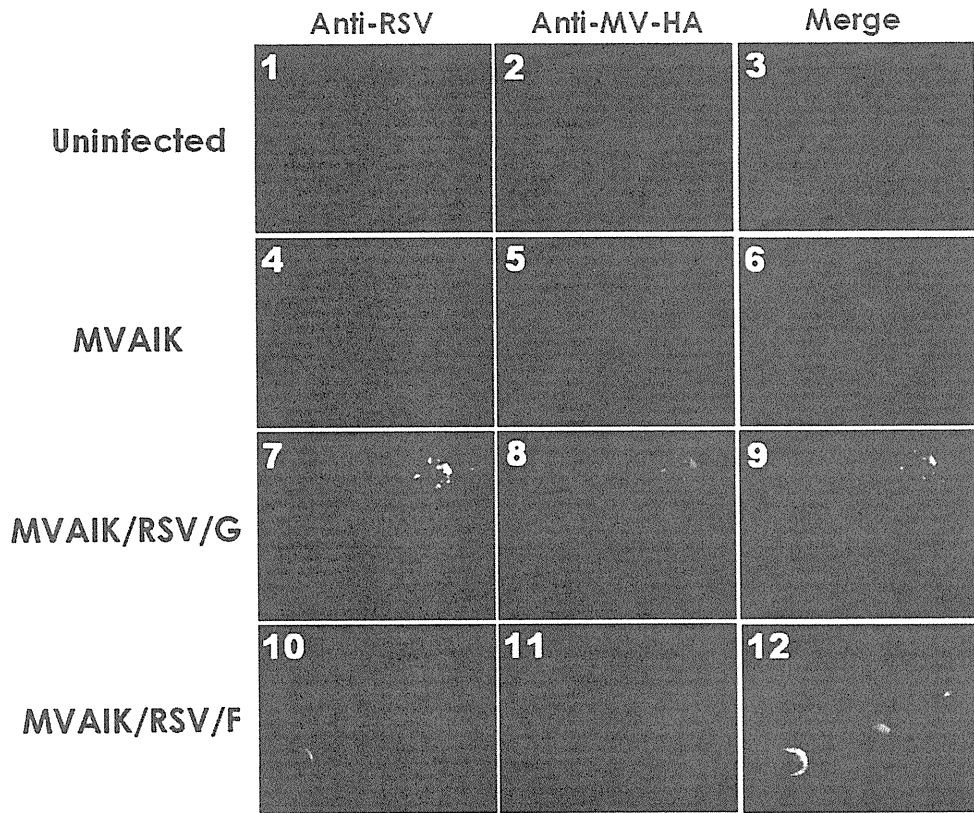
Fig. 4. Expression of MV HA and RSV G or F protein. B95a cells were infected with MVAIK (panels 4 and 5), MVAIK/RSV/G (panels 7 and 8) or MVAIK/RSV/F (panels 10 and 11) at a m.o.i. of 0.01 in 24-well plate and cultured for two days at 33 C. Uninfected B95a cells are shown in panels 1 and 2. B95a cells were collected and subjected to live cell staining without fixation to detect the surface expression. The expression of RSV (panels 1, 4, 7, and 10) and MV HA protein (panels 2, 5, 8, and 11) are shown. Panels 3, 6, 9 and 12 are merged images.
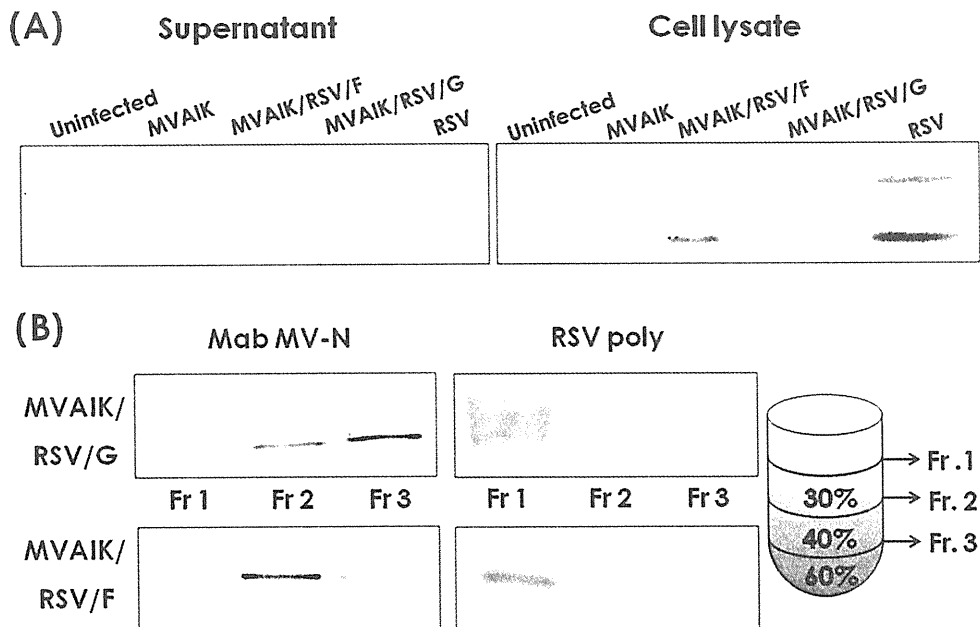
Fig. 5. Results of Western blotting of culture supernatant, cell lysate, and purified recombinant measles viral particles. (A) Vero cells were infected with MVAIK, MVAIK/RSVF, and MVAIK/RSV/G and HEp-2 cells were infected with RSV subgroup A, Long strain, and were cultured in 1 ml in a 24-well plate. Just before the appearance of CPE, culture media was replaced with serum free medium (VP-SFM). 1 ml of culture medium was harvested and 100 µl of PBS was added in plate. Cells were freeze-thawed and cell lysate was clarified. As for the Western blotting, 1/30 of initial supernatants and 1/100 of cell lysate were subjected for experiments. They were stained with polyclonal antibodies against RSV. (B) Infectious particles were obtained through sucrose discontinuous gradient ultra-centrifugation. Fraction 1 was obtained at the top of the gradient of 30% sucrose, Fraction 2 between 30% and 45% sucrose, and Fraction 3 between 45% and 60% sucrose. Each fraction was analyzed by Western blotting, using RSV polyclonal antibodies and monoclonal antibodies against MV N protein.
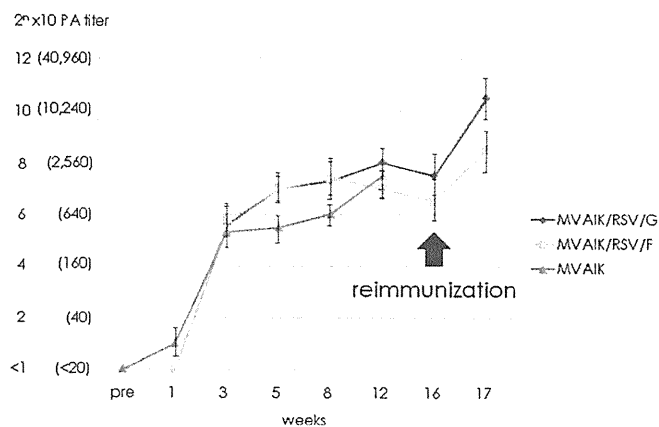
Fig. 6. Serological response of PA antibodies against MV. PA antibody titers were examined, using Serodia®-Measles. PA titers are expressed as $2^n \times 10$. Sera were collected before immunization, and 1, 3, 5, 8, 12, 16, and 17 weeks after immunization with MVAIK, MVAIK/RSV/G, and MVAIK/RSV/F. Five cotton rats were immunized and followed for 12 weeks. Mean PA titers ± 1.0 S.D. are shown. Two rats for each were reimmunized at the 16th week.

against the MV N protein. RSV G or F was detected in Fraction 1, and, whereas the MV N protein was detected in Fractions 2 and 3 (Fig. 5, Panel B). Accordingly, RSV G or F protein translated from the inserted gene was considered not to be incorporated into MV particles.

3.3. Immunogenicity of recombinant measles viruses

The recombinant viruses, MVAIK/RSV/G and MVAIK/RSV/F, were inoculated into cotton rats to confirm the immunogenicity intramuscularly of the inserted RSV G or F protein. Five cotton rats were immunized with MVAIK, MVAIK/RSV/G, and MVAIK/RSV/F for each study group and serum samples were obtained before and 1, 3, 5, 8, 12, and 16 weeks after immunization. The results are shown in Fig. 6. PA antibodies against MV were detected three weeks after the immunization in all animals. High levels of PA antibody, $2^{6-8} \times 10$ (1:640–1:2560), were maintained until 16th week in those immunized with MVAIK, MVAIK/RSV/G, and MVAIK/RSV/F. Two rats were reimmunized 16 weeks after the first immunization and sera were obtained one week after the reimmunization for each group. PA antibodies increased from $2^{7.5 \pm 1.5}$ to $2^{10.5 \pm 1.5} \times 10$ in the MVAIK/RSV/G group, and from $2^{6.5 \pm 1.5}$ to $2^{8.5 \pm 1.5} \times 10$ in the MVAIK/RSV/F group. PA antibodies against MV increased after the reimmunization by four to eight-fold.

The results for NT antibodies against RSV are shown in Fig. 7. In the cotton rats immunized with MVAIK/RSV/G, NT antibodies against RSV subgroup A were detected one week after immunization but the mean titer began to decrease 5 week after immunization. The mean NT titers against RSV subgroup A decreased to undetectable levels 12 weeks after the immunization. In the MVAIK/RSV/F group, NT antibodies against RSV subgroup A were detected one week after the immunization in all animals with a mean titer of $10^{2.0 \pm 0.7}$. High titers were observed at the 5th week with a mean of $10^{2.6 \pm 1.0}$. Levels of these antibodies were maintained until 16th week.

In this experiment, RSV source of the recombinant MVAIK/RSV/F or MVAIK/RSV/G was derived from the RSV subgroup A wild type. Cross immunity against RSV subgroup B was further investigated. In cotton rats immunized with MVAIK/RSV/F, NT antibodies against RSV subgroup B were detected at the 3rd week with a mean titer of 150 ($10^{2.1}$) and maintained for 16 weeks. However, cross-reactive antibodies against RSV subgroup B were not detected in the cotton rats immunized with MVAIK/RSV/G.
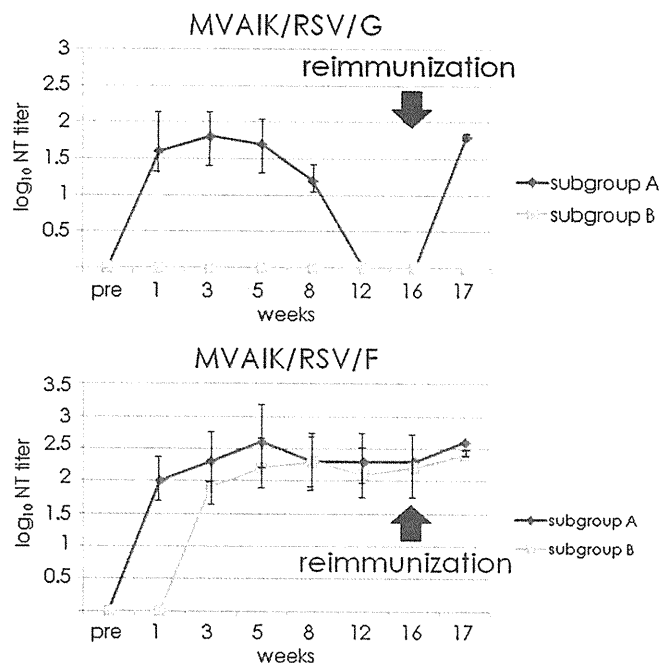
Fig. 7. Development of NT antibodies against RSV. NT antibodies were examined using the RSV Long strain (Subgroup A) and wild-type RSV subgroup B strain. Sera were collected before immunization, and 1, 3, 5, 8, 12, 16, and 17 weeks after immunization. 50% plaque reduction NT titers are expressed 10^n and are shown as mean NT titers with 1.0 S.D. The upper panel shows the immune response after immunization with MVAIK/RSV/G. The lower panel shows the results after immunization with MVAIK/RSV/F.

In the cotton rats immunized with MVAIK/RSV/F, NT antibodies against RSV subgroups A and B increased after reimmunization by two fold, but not significantly. As for the rats immunized with MVAIK/RSV/G, NT antibodies against RSV subgroup A were boosted from an undetectable level before the reimmunization to $10^{1.8 \pm 0.1}$ but those against RSV subgroup B were not detected.
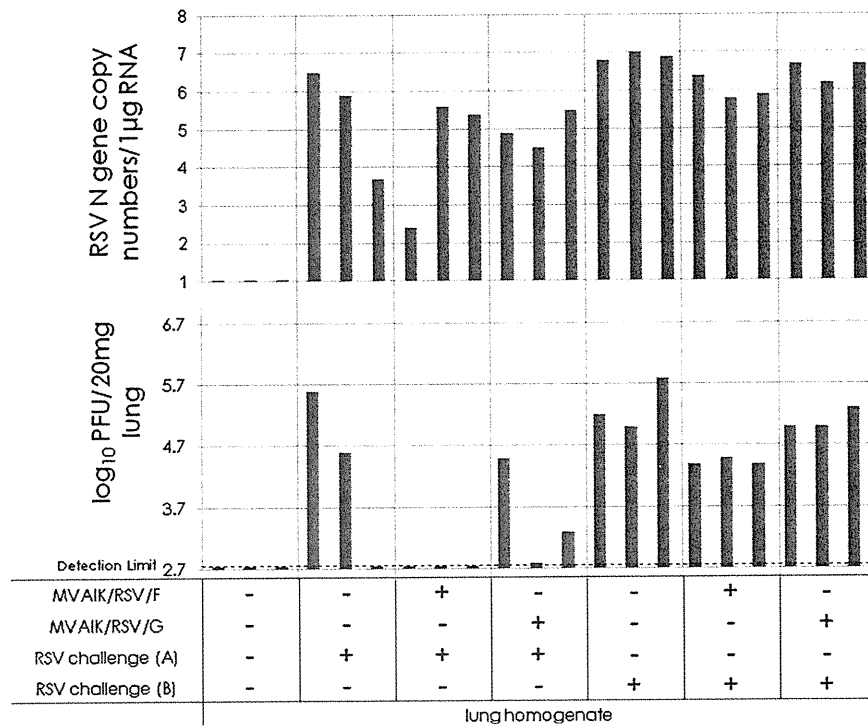
3.4. Protection against RSV challenge

The peak response against RSV was observed five weeks after immunization. Three cotton rats were immunized with MVAIK/RSV/F and MVAIK/RSV/G and challenged with the homologous RSV subgroup A (Long strain) and heterologous subgroup B (wild-type). No infectious virus was recovered from nasal wash and BAL but RSV genome was detected. RSN genome copy number was slightly lower in immunized groups but not significant (data not shown). The recovery of infectious virus and genome copy numbers from lung tissues are shown in Fig. 8. $10^{5.4}$ and $10^{4.5}$ PFU of infectious virus were recovered from 20 mg of lung tissue in two cotton rats of the control group challenged with RSV subgroup A, but no infectious virus was recovered in three cotton rats immunized with MVAIK/RSV/F. Meanwhile, $10^{4.5}$, $10^{2.8}$ and $10^{3.3}$ PFU of infectious virus were recovered in cotton rats immunized with MVAIK/RSV/G.

As for challenge with RSV subgroup B, $10^{5.0-5.8}$ PFU of RSV was recovered from lung infected with RSV subgroup B in non-immunized rats. In cotton rats immunized with MVAIK/RSV/F, virus titers were slightly lower, $10^{4.4-4.5}$ PFU but $10^{5.0-5.3}$ PFU from their lung tissues in the cotton rats immunized with MVAIK/RSV/G. There was no significant reduction in RSV N gene copy number.

For histopathological examinations, lung tissues were obtained four days after the challenge with RSV subgroups A and B and the results of HE staining and immuno-staining against RSV antigens are shown in Fig. 9. The non-immunized rat challenged with RSV subgroup A showed prominent interstitial pneumonia

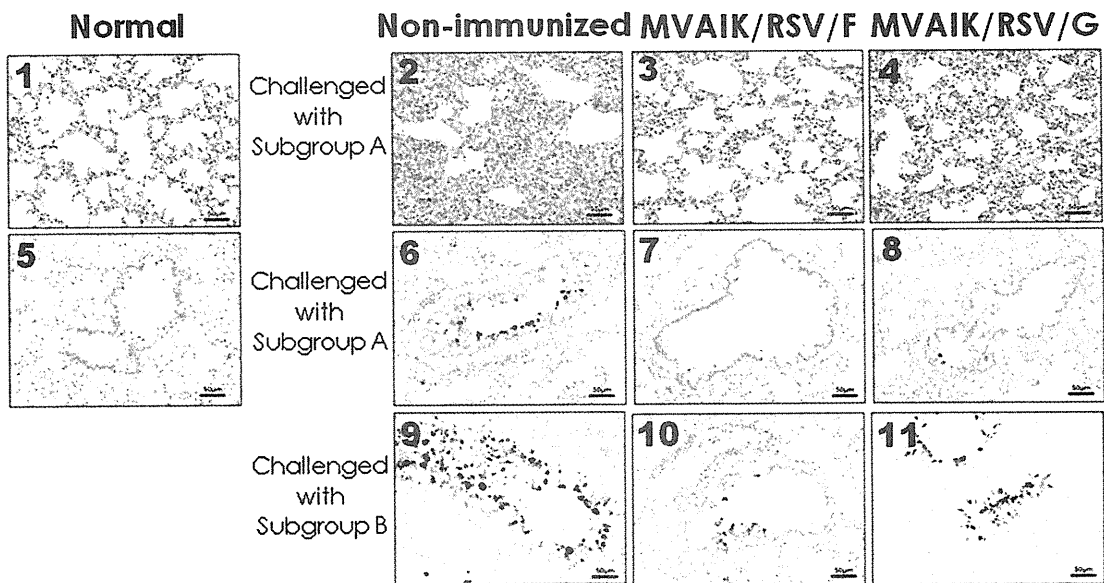| MVAIK/RSV/F | – | – | + | – | – | + | – |
MVAIK/RSV/G	–	–	–	+	–	–	+
RSV challenge (A)	–	+	+	+	–	–	–
RSV challenge (B)	–	–	–	–	+	+	+

lung homogenate

Fig. 8. Recovery of RSV infectious virus and genome copy numbers after challenge with RSV subgroups A and B. Three cotton rats were investigated in the normal control group, non-immunized group, and group immunized with MVAIK/RSV/F or MVAIK/RSV/G. Animals non-immunized group, and group immunized with MVAIK/RSV/F or MVAIK/RSV/G were challenged with 1.0×10^6 PFU of the homologous RSV Long strain and wild-type subgroup B five weeks later. Virus infectivity was monitored in lung homogenate, and RSV infectivity is shown as PFU in 20 mg of lung tissue. And 1 µg of total RNA of lung tissue was used for real-time PCR, and each column represents individual result.

(panel 2; thickening of alveolar wall, and infiltration of inflammatory mononuclear cells) with RSV antigens in bronchial epithelial cells (panel 6). In cotton rat immunized with MVAIK/RSV/F showed very mild inflammation (panel 3), though most sections were normal, without RSV antigen in bronchial tissue after RSV challenge with subgroup A (panel 7). In cotton rat immunized with MVAIK/RSV/G, moderate interstitial pneumonia was

observed with a small amount of RSV antigen (panels 4 and 8).

As for the challenge with RSV subgroup B, histological findings in non-immunized rat challenged with subgroup B were similar to the results challenged with RSV subgroup A. The results of immuno-staining are shown. Large amounts of RSV antigen were detected in non-immunized rat (panel 9). Small amounts of RSV antigens were

Fig. 9. Pulmonary histopathology in cotton rats challenged with RSV subgroups A and B. Cotton rats were immunized intramuscularly with MVAIK/RSV/F (panels 3, 7, and 10) or MVAIK/RSV/G (panels 4, 8, and 11) and then challenged five weeks later, with RSV subgroup A (panels 2, 3, 4, 6, 7, and 8) and subgroups B (panels 9, 10 and 11). They were sacrificed four days after the challenge. Histological examination was performed by HE staining of lung tissues (panels 1, 2, 3, and 4) and the results of immuno-staining of bronchiolar regions are shown in panels 5, 6, 7, 8, 9, 10, and 11. Immuno-staining was performed using four clone blend monoclonal antibodies against RSV P, F, and N proteins and anti-mouse IgG conjugated with HRP. HE staining and immuno-staining of normal control are shown in panels 1 and 5.

detected in MVAIK/RSV/F group (panel 10) in comparison with MVAIK/RSV/G group (panel 11). Finding of RSV antigens were well correlated with the results of the recovery of infectious virus from lung tissues. Inoculated virus would be cleared and demonstrated a mild pathological finding in rats immunized with MVAIK/RSV/F.

4. Discussion

RSV is a clinically important cause of respiratory tract infections, especially among high-risk infants, immunocompromised hosts, and the elderly. Despite a serious disease burden, there is no licensed vaccine for RSV. Initial efforts to develop a vaccine involved FI-RSV which unexpectedly enhanced the disease in clinical trials in RSV-naive children [33]. FI-RSV failed to induce a secretory IgA response after pareteral administration without inducing a CTL response, which was a serious drawback of the inactivated vaccine. The defeated F protein would not induce Th1 response and the aluminium-precipitated vaccine induced only Th2 response. The allergic reaction to this vaccine would be caused by the Th2-prone reaction [34]. Several subunit vaccines were investigated, but failed to generate effective antibodies. A live attenuated vaccine has the advantage of inducing humoral and cellular immune responses similar to a natural infection. Temperature-sensitive (ts) and cold-adapted (ca) RSV vaccine strains have been developed by conventional attenuation methods. Over the last 40 years, cautious and deliberate progress has been made toward developing a RSV vaccine using various experimental approaches, including live attenuated strains and vector-based and viral protein subunit vaccine candidates. But the balance between the safety and immunogenicity is a key issue to the development of a live attenuated vaccine, and the (ts) RSV vaccine candidate resulted in insufficient attenuation, causing similar respiratory illness [35]. Based on a vaccine candidate having the ts phenotype, several recombinant vaccine candidates were developed by deletion of the SH gene or NS1 gene or mutation by reverse genetics. These recombinant RSV vaccines induced sufficient immune response in chimpanzees [36]. Another approach involved the application of reverse genetics to express RSV protein in a recombinant vector-based vaccine. The first vector-based candidate was evaluated using vaccinia virus. Recombinants expressing RSV F or G was highly immunogenic, induced protection in mouse but provided inconsistent protection in chimpanzees [37]. MVA strain of vaccinia-based recombinants expressing RSV G and F protein were immunogenic in rodent but not in rhesus monkey model [38]. Several vector-based live vaccine platforms were established using HPIV-III and Sendai virus [23,39]. Through preceding experiments, the F protein is known to be more effective than G. But there were no experiences for clinical usage and the HPIV-III-based recombinant vaccine was poorly immunogenic in human clinical trials.

In this report, reverse genetics using the AIK-C live attenuated measles vaccines were developed. A recombinant measles virus vector-based vaccine was established using the Schwartz strain, expressing the West Nile virus [40]. As well as the Schwartz strain, the AIK-C measles vaccine is a further attenuated vaccine strain having the ts phenotype, and its safety and immunogenicity has been confirmed [26,29]. Thus, in this report, AIK-C was used for a live virus vaccine-vector. Expression of the RSV G or F protein was confirmed by indirect immuno-staining of B95a cells infected with MVAIK/RSV/G or F with polyclonal and monoclonal antibodies against the F protein. By Western blotting, the G or F protein was detected in culture medium and cell lysate of B95a cells infected with MVAIK/RSV/G or F. The RSV G and F proteins were considered not to be incorporated into MV particles because theoretically they had no binding site for the MV M protein. MV envelop proteins bound the M protein [41]. The genetic stability of the vaccine

candidate was examined and inserted genes for RSV G and F were stable even after 15 passages.

The recombinant measles virus (MVAIK) triggered an immune response three weeks after vaccination in cotton rats. Levels of these antibodies were maintained for 16 weeks. The same was observed after immunization with MVAIK/RSV/G or F. To investigate the viral growth, samples of nasal turbinate, lung, thymus, spleen, liver, kidney, and bone marrow were obtained 10 days after immunization, but no infectious virus was recovered. Total RNA was extracted and RT-real time PCR was performed to detect the measles N gene by real-time PCR. The MV genome was detected only in thymus in cotton rats immunized with MVAIK, MVAIK/RSV/G, and MVAIK/RSV/F (data not shown). Infectious virus was recovered from inguinal superficial lymph nodes three days after infection in the previous study [42]. NT antibody titers against RSV were investigated, using RSV Long (subgroup A) and wild-type subgroup B. MVAIK/RSV/G or MVAIK/RSV/F induced the production of NT antibodies against RSV subgroup A from one week after vaccination in cotton rats. Antibody titers were higher after immunization with MVAIK/RSV/F than with MVAIK/RSV/G. RSV has distinctly different subgroups, A and B. The G or F gene of subgroup A was used in this study. Therefore, the cross reaction of NT against subgroup B was investigated. MVAIK/RSV/G did not generate NT antibodies against RSV subgroup B, but MVAIK/RSV/F induced production of cross-reactive NT antibodies against RSV subgroups A and B. The predicted amino acid sequence of the RSV F protein used in this study exhibited 98.6% homology among F proteins of subgroup A strains and 90.8% in comparison with those of subgroup B strains. The predicted amino acid sequence of RSV G protein has 86.9% homology among subgroup A strains but 49.7% in comparison with subgroup B. Thus, F protein was relatively conserved between subgroups A and B but the G protein of RSV was variable and thought not suitable as a vaccine antigen. Recently, a humanized monoclonal antibody against the RSV F protein was used for prevention of serious RSV infections in young infants having cardiac and pulmonary disorders, with a low birth weight, or born prematurely. In this study, recombinant MVAIK/RSV/G or F was administered intramuscularly and induced sufficient NT antibodies. Secretory IgA antibodies and CTL response were not examined but it protected against the challenge with homologous RSV subgroup A. In non-immunized cotton rats, $10^{5.4}$ and $10^{4.5}$ PFU of infectious virus were recovered from 20 mg of lung tissue four days after the RSV challenge. But those immunized with MVAIK/RSV/F were protected, without recovery of infectious virus from the lung tissues. And they did not demonstrate interstitial pneumonia. Cross reactive NT antibodies were demonstrated after immunization with MVAIK/RSV/F but its protective effect is not sufficient against subgroup B, demonstrating slightly lower levels (approximately 1/10 of non-immunized control) of the recovery of infectious virus. Protective effects of MVAIK/RSV/G were poor in comparison with MVAIK/RSV/F similar to the serological responses.

As for the experimental animal models, transgenic mice expressing human CD46 with the knock out of type I interferon (IFN) receptor gene were used to evaluate the immunogenicity of a recombinant MV vaccine candidate produced using the West Nile virus [40], SARS corona virus [43], hepatitis B virus [44] and HIV [45]. Efficient immune responses were reported, but the IFN system is the most important signal for innate immunity. In the case of the RSV vaccine candidate, innate immunity modified the adaptive immunity, and, therefore, cotton rats without gene manipulation were used in these experiments [46].

Recombinant MV vaccine-based vectors have practical limitation for timing of immunization. In young infants, maternal conferred immunity would interfere with vaccine effects. In field trials, AIK-C gave efficient sero-conversion and induction of cell-mediated immunity even when the vaccine was given at the age

of six months [26,27]. They demonstrated more than 80% sero-conversion rate to overcome maternal conferred immunity and the safety was similarly confirmed, suggesting no evidence of immune-suppression. RSV infection was observed even after six months of age, and, therefore, MVAIK/RSV/F would be applicable for six months to provide protective immunity both against RSV and measles especially for developing countries.

As for the effective protection against RSV infection, intranasal administration is desired. But we have no experience of intranasal administration of AIK-C vaccine, and, in our previous experiments, the recombinant MVAIK did not induce serum NT against MV through intranasal administration because of the strict *ts* phenotype in cotton rat model, having high body temperature [21,42]. Therefore, the comparative studies are planning to investigate the immunogenicity and challenge tests in monkeys immunized with MVAIK/RSV/F.

In conclusion, a new MV vaccine-strain-based RSV vaccine candidate was demonstrated to confer protection against RSV in cotton rats. The xenogeneic recombinant might induce simultaneously protective immunity against backbone-MV and inserted-RSV infections. Recombinant MVAIK expressing RSV F protein is a promising candidate and protective effects should be confirmed in monkey model, considering the immunization routes.

Acknowledgements

References

[1] Lamb RA, Parks GD. *Paramyxoviridae*: the viruses and their replication. In: Knipe DM, Howley PM, editors. Fields virology. 5th ed. Philadelphia: Lippincott Williams & Wilkins; 2007. p. 1449–96.

[2] Collins PL, Hill MG, Camargo E, Grosfeld H, Chanock RM, Murphy BR. Production of infectious human respiratory syncytial virus from cloned cDNA confirms an essential role for the transcription elongation factor from the 5′ proximal open reading frame of the M2 mRNA in gene expression and provides a capability for vaccine development. Proc Natl Acad Sci USA 1995;92(25):11563–7.

[3] Chanock R, Finberg L. Recovery from infants with respiratory illness of a virus related to chimpanzee coryza agent (CCA). II. Epidemiologic aspects of infection in infants and young children. Am J Hyg 1957;66(3):291–300.

[4] Anderson LJ, Hierholzer JC, Tsou C, Hendry RM, Fernie BF, Stone Y, et al. Antigenic characterization of respiratory syncytial virus strains with monoclonal antibodies. J Infect Dis 1985;151(4):626–33.

[5] La Via WV, Grant SW, Stutman HR, Marks MI. Clinical profile of pediatric patients hospitalized with respiratory syncytial virus infection. Clin Pediatr (Phila) 1993;32(8):450–4.

[6] Henderson FW, Collier AM, Clyde Jr WA, Denny FW. Respiratory-syncytial-virus infections, reinfections and immunity. A prospective, longitudinal study in young children. N Engl J Med 1979;300(10):530–4.

[7] Ebbert JO, Limper AH. Respiratory syncytial virus pneumonitis in immunocompromised adults: clinical features and outcome. Respiration 2005;72(3):263–9.

[8] Anderson LJ, Parker RA, Strikas RL. Association between respiratory syncytial virus outbreaks and lower respiratory tract deaths of infants and young children. J Infect Dis 1990;161(4):640–6.

[9] González PA, Bueno SM, Riedel CA, Kalergis AM. Impairment of T cell immunity by the respiratory syncytial virus: targeting virulence mechanisms for therapy and prophylaxis. Curr Med Chem 2009;16(34):4609–25.

[10] Becker Y. Respiratory syncytial virus (RSV) evades the human adaptive immune system by skewing the Th1/Th2 cytokine balance toward increased levels of Th2 cytokines and IgE, markers of allergy—a review. Virus Genes 2006;33(2):235–52.

[11] Fisher RG, Crowe Jr JE, Johnson TR, Tang YW, Graham BS. Passive IgA monoclonal antibody is no more effective than IgG at protecting mice from mucosal challenge with respiratory syncytial virus. J Infect Dis 1999;180(4):1324–7.

[12] Piedra PA, Cron SG, Jewell A, Hamblett N, McBride R, Palacio MA, et al. Immunogenicity of a new purified fusion protein vaccine to respiratory syncytial virus: a multi-center trial in children with cystic fibrosis. Vaccine 2003;21(19–20):2448–60.

[13] Lofland JH, O'Connor JP, Chatterton ML, Moxey ED, Paddock LE, Nash DB, et al. Palivizumab for respiratory syncytial virus prophylaxis in high-risk infants: a cost-effectiveness analysis. Clin Ther 2000;22(11):1357–69.

[14] Murphy BR, Prince GA, Walsh EE, Kim HW, Parrott RH, Hemming VG, et al. Dissociation between serum neutralizing and glycoprotein antibody responses of infants and children who received inactivated respiratory syncytial virus vaccine. J Clin Microbiol 1986;24(2):197–202.

[15] Murphy BR, Walsh EE. Formalin-inactivated respiratory syncytial virus vaccine induces antibodies to the fusion glycoprotein that are deficient in fusion-inhibiting activity. J Clin Microbiol 1988;26(8):1595–7.

[16] Wright PF, Belshe RB, Kim HW, Van Voris LP, Chanock RM. Administration of a highly attenuated, live respiratory syncytial virus vaccine to adults and children. Infect Immun 1982;37(1):397–400.

[17] Whitehead SS, Firestone CY, Karron RA, Crowe Jr JE, Elkins WR, Collins PL, et al. Addition of a missense mutation present in the L gene of respiratory syncytial virus (RSV) cpts530/1030 to RSV vaccine candidate cpts248/404 increases its attenuation and temperature sensitivity. J Virol 1999;73(2):871–7.

[18] Collins PL, Purcell RH, London WT, Lawrence LA, Chanock RM, Murphy BR. Evaluation in chimpanzees of vaccinia virus recombinants that express the surface glycoproteins of human respiratory syncytial virus. Vaccine 1990;8:164–8.

[19] Nakayama T, Komase K, Uzuka R, Hoshi A, Okafuji T. Leucine at position 278 of the AIK-C measles virus vaccine strain fusion protein is responsible for reduced syncytium formation. J Gen Virol 2001;82:2143–50.

[20] Ballart I, Eschle D, Cattaneo R, Schmid A, Metzler M, Chan J, et al. Infectious measles virus from cloned cDNA. EMBO J 1990;9(2):379–84.

[21] Komase K, Nakayama T, Iijima M, Miki K, Kawanishi R, Uejima H. The phosphoprotein of attenuated measles AIK-C vaccine strain contributes to its temperature-sensitive phenotype. Vaccine 2006;24(6):826–34.

[22] Tang RS, MacPhail M, Schickli JH, Kaur J, Robinson CL, Lawlor HA, et al. Parainfluenza virus type 3 expressing the native or soluble fusion (F) protein of respiratory syncytial virus (RSV) confers protection from RSV infection in African green monkeys. J Virol 2004;78(20):11198–207.

[23] Zhan X, Hurwitz JL, Krishnamurthy S, Takimoto T, Boyd K, Scroggs RA, et al. Respiratory syncytial virus (RSV) fusion protein expressed by recombinant Sendai virus elicits B-cell and T-cell responses in cotton rats and confers protection against RSV subtypes A and B. Vaccine 2007;25(52):8782–93.

[24] Rima BK, Earle JA, Yeo RP, Herlihy L, Baczko K, ter Meulen V, et al. Temporal and geographical distribution of measles virus genotypes. J Gen Virol 1995;76(Pt 5):1173–80.

[25] Makino S, Sasaki K, Nakamura N, Nakagawa M, Nakajima S. Studies on the modification of the live AIK measles vaccine. II. Development and evaluation of the live AIK-C measles vaccine. Kitasato Arch Exp Med 1974;47(1–2):13–21.

[26] Bolotovski VM, Grabowsky M, Clements CJ, Albrecht P, Brenner ER, Zargaryantzs AI, et al. Immunization of 6 and 9 month old infants with AIK-C, Edmonston-Zagreb, Leningrad-16 and Schwarz strains of measles vaccine. Int J Epidemiol 1994;23(5):1069–77.

[27] Pabst HF, Spady DW, Carson MM, Krezolek MP, Barreto L, Wittes RC. Cell-mediated and antibody immune responses to AIK-C and Connaught monovalent measles vaccine given to 6 month old infants. Vaccine 1999;17(15–16):1910–8.

[28] Cutts FT, Grabowsky M, Markowitz LE. The effect of dose and strain of live attenuated measles vaccines on serological responses in young infants. Biologicals 1995;23(1):95–106.

[29] Nakayama T, Onoda K. Vaccine adverse events reported in post-marketing study of the Kitasato Institute from 1994 to 2004. Vaccine 2007;25(3):570–6.

[30] Kobune F, Sakata H, Sugiura A. Marmoset lymphoblastoid cells as a sensitive host for isolation of measles virus. J Virol 1990;64(February (2)):700–5.

[31] Kumada A, Komase K, Nakayama T. Recombinant measles AIK-C strain expressing current wild-type hemagglutinin protein. Vaccine 2004;22(3–4):309–16.

[32] Sutter G, Ohlmann M, Erfle V. Non-replicating vaccinia vector efficiently expresses bacteriophage T7 RNA polymerase. FEBS Lett 1995;371(1):9–12.

[33] Kapikian AZ, Mitchell RH, Chanock RM, Shvedoff RA, Stewart CE. An epidemiologic study of altered clinical reactivity to respiratory syncytial (RS) virus infection in children previously vaccinated with an inactivated RS virus vaccine. Am J Epidemiol 1969;89(4):405–21.

[34] Polack FP, Teng MN, Collins PL, Prince GA, Exner M, Regele H, et al. A role for immune complexes in enhanced respiratory syncytial virus disease. J Exp Med 2002;196(6):859–65.

[35] Karron RA, Wright PF, Crowe Jr JE, Clements-Mann ML, Thompson J, Makhene M, et al. Evaluation of two live, cold-passaged, temperature-sensitive respiratory syncytial virus vaccines in chimpanzees and in human adults, infants, and children. J Infect Dis 1997;176(6):1428–36.

[36] Teng MN, Whitehead SS, Bermingham A, St Claire M, Elkins WR, Murphy BR, et al. Recombinant respiratory syncytial virus that does not express the NS1 or M2-2 protein is highly attenuated and immunogenic in chimpanzees. J Virol 2000;74(19):9317–21.

[37] Wyatt LS, Whitehead SS, Venanzi KA, Murphy BR, Moss B. Priming and boosting immunity to respiratory syncytial virus by recombinant replication-defective vaccinia virus MVA. Vaccine 1999;18(5–6):392–7.

[38] de Wall L, Wyatt LS, Yuksel S, Van Amerongen G, Moss B, Niester HG, et al. Vaccination of infant macaques with a recombinant modified vaccinia virus Ankara expressing the respiratory syncytial virus F and G genes does not predispose for immunopathology. Vaccine 2004;22:923–6.

[39] Jones B, Zhan X, Mishin V, Slobod KS, Surman S, Russell CJ, et al. Human PIV-2 recombinant Sendai virus (rSeV) elicits durable immunity and combines with

two additional rSeVs to protect against hPIV-1, hPIV-2, hPIV-3, and RSV. Vaccine 2009;27(12):1848–57.

[40] Desprès P, Combredet C, Frenkiel MP, Lorin C, Brahic M, Tangy F. Live measles vaccine expressing the secreted form of the West Nile virus envelope glycoprotein protects against West Nile virus encephalitis. J Infect Dis 2005;191(2):207–14.

[41] Wild TF, Buckland R. Functional aspects of envelope-associated measles virus proteins. Curr Top Microbiol Immunol 1995;191:51–64.

[42] Haga T, Murayama N, Shimizu Y, Saito A, Sakamoto T, Morita T, et al. Analysis of antibody response by temperature-sensitive measles vaccine strain in the cotton rat model. Comp Immunol Microbiol Infect Dis 2009;32(5):395–406.

[43] Liniger M, Zuniga A, Tamin A, Azzouz-Morin TN, Knuchel M, Marty RR, et al. Induction of neutralising antibodies and cellular immune responses against SARS coronavirus by recombinant measles viruses. Vaccine 2008;26(17):2164–74.

[44] del Valle JR, Devaux P, Hodge G, Wegner NJ, McChesney MB, Cattaneo R. A vectored measles virus induces hepatitis B surface antigen antibodies while protecting macaques against measles virus challenge. J Virol 2007;81(19):10597–605.

[45] Liniger M, Zuniga A, Morin TN, Combardiere B, Marty R, Wiegand M, et al. Recombinant measles viruses expressing single or multiple antigens of human immunodeficiency virus (HIV-1) induce cellular and humoral immune responses. Vaccine 2009;27(25–26):3299–305.

[46] Boukhvalova MS, Prince GA, Blanco FCG. The cotton rat model of respiratory viral infections pathogenesis and immunity. Biologicals 2009;37: 152–9.

Amino Acid Substitutions in Matrix, Fusion and Hemagglutinin Proteins of Wild Measles Virus for Adaptation to Vero Cells

Ji Yi Xin[a, b]   Toshiaki Ihara[c]   Katsuhiro Komase[d]   Tetsuo Nakayama[b]

[a]National Laboratory for Measles, National Institute for Viral Disease Control and Prevention, Chinese Center for Disease Control and Prevention, Beijing, China; [b]Laboratory of Viral Infection I, Kitasato Institute for Life Sciences, Kitasato University, Tokyo, [c]Department of Pediatrics, National Mie Hospital, Tsu, and [d]Laboratory of Measles Viruses, Department of Virology III, National Institute of Infectious Diseases, Musashimurayama, Japan

Abstract

Background: Wild-type measles virus (MV) is isolated in B95a but not in Vero cells. Through an adaptation process of wild-type MV to Vero cells, several amino acid substitutions were reported. ***Methods:*** Six strains were adapted to Vero cells and membrane (M), fusion (F) and hemagglutinin (H) genes were sequenced. Cell fusion was assessed and recombinant MVs were constructed, having wild-type H or M gene with or without mutations. ***Results:*** No F gene substitution was noted. Amino-acid substitutions at positions 481 from Asn to Tyr (N481Y) and 546 from Ser to Gly (S546G) were observed in the H protein. Glu at position 89 of the M protein was substituted for Gly (E89G) and two mutations were noted at positions 62 (S62R) and 83 (S83P) in M protein. Recombinant viruses with mutation(s) detected in Vero-adapted strains induced a cytopathic effect and grew well in Vero cells, but those with the wild type did not. Recombinant viruses with mutation(s) demonstrated lower viral growth in B95a cells. ***Conclusions:*** Substitutions of E89G, S62R and S83P of the M protein were newly observed through adaptation to Vero cells, besides the mutations described in previous reports, with varying adaptation for each strain.

Copyright © 2011 S. Karger AG, Basel

Introduction

Measles virus (MV) is a member of the genus *Morbillivirus*, family Paramyxoviridae, order Mononegavirales, characterized by non-segmented, negative-strand RNA virus. The genome consists of 15,894 nucleotides, coding six structural proteins: nucleoprotein (N), phospho (P), membrane (M), fusion (F), hemagglutinin (H) and large (L) proteins. The genomic RNA is encapsidated with N protein and consisted of ribonucleoprotein, together with RNA-dependent RNA polymerase complex of L and P proteins [1, 2]. MV has two envelop glycoproteins, F and H, which play an important role in virus attachment and subsequent virus cell fusion as well as cell-to-cell fusion [3–5]. The Edmonston strain was isolated in 1954 using a primary culture of human kidney cells and, thereafter, MV was isolated using Vero cells, but the sensitivity of Vero cells was poor, and two or three blind passages were required. MV was isolated more efficiently in B95a cells, marmoset lymphoblastic cell lines transformed by Epstein-Barr virus [6]. CD46 was initially reported to act as a cellular receptor for laboratory-adapted, vaccine strains of MV. CD46 is a member of the regulators of the complement activation gene cluster and is widely expressed on epithelial cells, but not on lymphocytic cells [7, 8]. In 2000, human signaling lymphocyte activation molecule (SLAM; CD150) was reported as the receptor of wild-type MV and it was expressed on lymphocytic cells [9, 10]. The

Tetsuo Nakayama, MD
Laboratory of Viral Infection I
Kitasato Institute for Life Sciences, Kitasato University
Shirokane 5-9-1, Minato-ku, Tokyo 108-8641 (Japan)
Tel. +81 3 5791 6269, Fax +81 3 5791 6130, E-Mail tetsuo-n@lisci.kitasato-u.ac.jp

Edmonston strain and relevant vaccine strains were found to use both SLAM and CD46 as receptors and circulating wild-type strains utilize SLAM as a receptor, but not CD46 [9, 10].

Several amino-acid changes in H, M, L and P proteins and/or accessory V and C proteins were responsible for attenuation through adaptation to Vero cells. Some authors reported that the majority of MV strains using CD46 as a receptor have tyrosine at position 481, whereas wild-type strains have asparagine at this position [11–17]. When the wild-type MV strains became adapted to grow in Vero cells, the substitution at position 481 of H protein from asparagine to tyrosine (N481Y) was often observed after several passages [16, 18]. In some Vero cell-adapted strains, a substitution at position 546 of the H protein from serine to glycine (S546G) was observed instead of the N481Y substitution [19–22]. A single substitution of N481Y or S546G enabled the H protein of wild-type MV strains to utilize CD46, without influencing their ability to use SLAM. In addition, two amino-acid differences were observed in Edmonston-derived strains in comparison with wild-type strains at positions 64 and 89 of M protein (P64S and E89K), which allowed an interaction of M protein with the cytoplasmic tail of H protein, thereby enhancing cell fusion and assembly of infectious particles in Vero cells [23–25].

In this report, amino-acid substitutions were investigated in M, F and H proteins of Vero-adapted strains from six wild-type MV strains isolated in B95a cells, in comparison with the original wild types. Mutations of N481Y or S546G of the H protein region were observed as previously reported. In addition, mutations in S62R, S83P and E89G of the M protein region were noted, being different from the mutations described in previous reports. Recombinant MV strains with mutations in the H and M genes were constructed to conduct a functional analysis of the mutations.

Materials and Methods

Cells and Viruses

Six strains of the wild type were used in this study. MVi/Tokyo.JPN/17.07-AN/B4, MVi/Mie.JPN/19.07-OY/B4, MVi/Mie.JPN/23.07-TY/B3, MVi/Mie.JPN/41.07-MA/B3 and MVi/Mie.JPN/03.08-KU/B4 were genotype D5 isolated in 2007/2008 outbreaks in Japan, using B95a cells after three or four passages. MVi/Aichi.JPN/44.06/B3 was genotype D9 [26]. Through several passages in Vero cells, eight Vero-adapted strains were obtained. AN-V4 was obtained after four passages of MVi/Tokyo.JPN/17.07-AN/B4 in Vero cells. OY-V4 and OY-V22 were obtained after four and 22 passages of MVi/Mie.JPN/19.07-OY/

B4 in Vero cells, respectively. TY-V4, TY-V22, MA-V15, KU-V4 and D9-V4 strains were obtained after passages of respective strains in Vero cells. MVAT7 pol., non-replicative vaccinia virus expressing T7 RNA polymerase (a kind gift from Dr. G. Sutter), was used for fusion analysis and the recovery of infectious viruses.

B95a cells were maintained in RPMI 1640 medium supplemented with 10% fetal calf serum (FCS), and Vero cells in MEM supplemented with 5% FCS. 293 T cells were cultured in MEM supplemented with 10% FCS.

Construction of F and H Expression Plasmids and Fusion Experiment

The H protein expression plasmids were constructed from Vero-adapted strains (AN-V4, OY-V4, OY-V22, TY-V22, MA-V15, KU-V4 and D9-V4 strains) and their original wild-type isolates and AIK-C strain. The H gene was amplified by RT-PCR using the set of primers H-ATG (5'-GTT<u>GAATTC</u>ATGTCACCAC-AACGAGACCGGA-3') and H-TAG (5'-AAT<u>GCGGCCGC</u>CT-ATCTGCGATTGGTTCCA-3'), containing restriction enzyme sites of EcoRI and NotI (underlined). The amplified DNA fragments were cloned into multicloning sites located downstream of the T7 promoter of pBluescript SK II–. Several clones were sequenced to analyze the frequency of mutations. Constructed H expression plasmid (0.2 μg) was co-transfected together with the AIK-C F expression plasmid into a monolayer of B95a or Vero cells infected with recombinant vaccinia virus, MVAT7 pol., using Mirus Superfect III (Invitrogen Life Technologies, Carlsbad, Calif., USA) [27]. Cells were fixed with cooled acetone and further subjected to indirect immunofluorescent (IF) staining.

Construction of Recombinant MV Strains with Mutations

The infectious recombinant MV strains were recovered from the infectious cDNA clone based on the AIK-C measles vaccine strain, expressing wild-type measles H protein cloned from the wild-type MV [27, 28], and the recombinant infectious cDNA constructions are shown in figure 1. Briefly, full-length cDNA of the AIK-C strain was divided into two parts: the first half consisted of AIK-C cDNA from the leader to the PacI site at nucleotide position 7238 of the AIK-C genome, and the second half of the AIK-C cDNA consisted of H and L regions from the 7239 PacI site to the trailer sequence. The AscI site (<u>GGCGCGCC</u>) was artificially introduced by adding a GGCGCG sequence upstream of the genome position 3433 in the P/M junction, and R1 and R2 sequences were added. The green fluorescent protein (GFP) sequence was inserted using NcoI and NotI restriction enzyme sites in accordance with the rule of six of the genome length [29, 30], designated as pMVAIK P/M-GFP. The H gene of the wild-type or Vero-adapted strains was cloned at NheI (genome position 7426) and PvuII (genome position 9082) of the second half of the AIK-C cDNA and combined with the first half of the cDNA. The M gene of the wild-type or Vero-adapted strains was cloned at BglII (genome position 3445) and BanIII (genome position 4312) sites of the first half of the AIK-C cDNA clone and combined with the second half to construct full-length cDNA.

For the recovery of the recombinant MV, 293 T cells were infected with MVAT7 pol., and then 0.5 μg of pAIK-N, 0.25 μg of pAIK-P, 0.1 μg of pAIK-L and 1.5 μg of full-length recombinant cDNA, using Mirus Superfect III (Invitrogen Life Technologies) modified from previous reports [27, 28]. After 2 days of culture,